



저작자표시-비영리-변경금지 2.0 대한민국

이용자는 아래의 조건을 따르는 경우에 한하여 자유롭게

- 이 저작물을 복제, 배포, 전송, 전시, 공연 및 방송할 수 있습니다.

다음과 같은 조건을 따라야 합니다:



저작자표시. 귀하는 원저작자를 표시하여야 합니다.



비영리. 귀하는 이 저작물을 영리 목적으로 이용할 수 없습니다.



변경금지. 귀하는 이 저작물을 개작, 변형 또는 가공할 수 없습니다.

- 귀하는, 이 저작물의 재이용이나 배포의 경우, 이 저작물에 적용된 이용허락조건을 명확하게 나타내어야 합니다.
- 저작권자로부터 별도의 허가를 받으면 이러한 조건들은 적용되지 않습니다.

저작권법에 따른 이용자의 권리는 위의 내용에 의하여 영향을 받지 않습니다.

이것은 [이용허락규약\(Legal Code\)](#)을 이해하기 쉽게 요약한 것입니다.

[Disclaimer](#)

**Thesis for the Degree of Master of Engineering**

**Measurement Method of Injury Rate on  
Fish Skin Using an Image Processing  
System**



**by**

**Minh Thien Tran**

**Department of Mechanical Design Engineering,  
The Graduate School**

**Pukyong National University**

**February 2019**

# **Measurement Method of Injury Rate on Fish Skin Using an Image Processing System**

**영상 처리시스템을 이용한 어체 피부  
손상을 측정법**

by

**Minh Thien Tran**

**Advisor: Professor Sang Bong Kim**

**A thesis submitted in partial fulfillment of the requirements for the  
degree of Master of Engineering**

**In the Department of Mechanical Design Engineering,  
The Graduate School,  
Pukyong National University**

**February 2019**

# Measurement Method of Injury Rate on Fish Skin Using an Image Processing System

A thesis

by

**Minh Thien Tran**

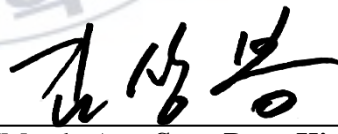
Approved as to styles and contents by:



(Chairman) **Jin Ho Suh**



(Member) **Il Yeong Lee**



(Member) **Sang Bong Kim**

February 2019

## **Acknowledgements**

Foremost, I would like to express my sincere gratitude to my advisor, Professor Sang Bong Kim, for the continuous support of my Master degree courses and research, his immense knowledge, motivation, patience, and his enthusiasm. Prof. Kim has been an adviser, financial supporter and strong motivator for my research of two years. His guidance and ideas helped me to accomplish my research and finish my thesis scientifically.

I would like to thank Professor Jin Ho Suh, Professor Ill Yeong Lee who have provided wonderful feedback and great suggestions for my thesis.

I would like to thank Prof. Hak Kyeong Kim for his guidance, tremendous encouragement and great helps to research and complete my thesis. I could not finish my thesis soon without his great help.

I am grateful to Prof. Tan Tien Nguyen from Ho Chi Minh City University of Technology for his essential assistances.

I would like to give special thank Dr. Huy Hung Nguyen, Dr. Trong Hai Nguyen and Dr. Van Tu Duong who have provided wonderful knowledge, great suggestions and practical experiences for my study in Korea.

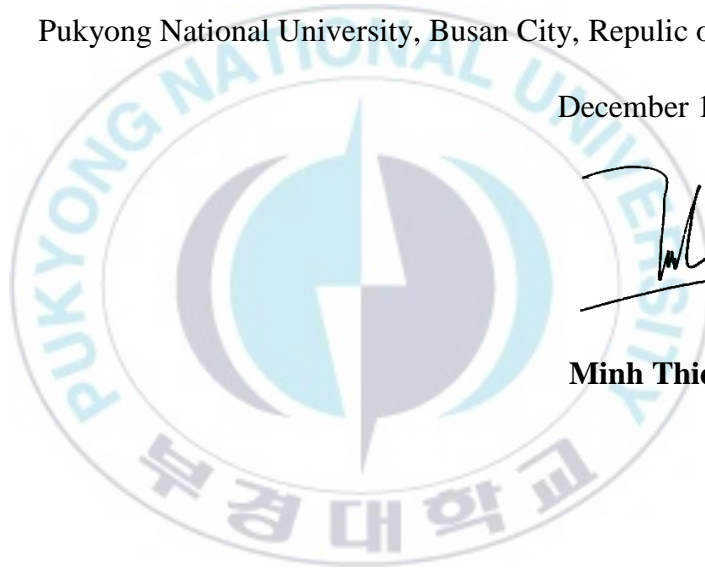
I would like to thank all members of Computer Integrated Manufacturing Electronics Commerce Laboratory (CIMEC Lab): Mr. Jotje Rantung, Mr. Van Lanh Nguyen, Mr. Chang Kyu Kim, Mr. Jong Min Oh, Mr. Sung Won Kim, Mr. Sung Rak Kim, Mr. Dong Yeong Kim and Ms. Hee Young Kim for all their helps, cooperation, encouragements and friendship.

I thank Vietnamese students of Marine Cybernetics Laboratory in Dept. of Mechanical System Engineering for their advices and supports.

Last but not least, I owe more than thanks to my parents, my wife, my brothers and all my close relatives for their encouragement throughout my life. Without their supports, there will be a lot of difficulties for me to finish my graduated study completely.

Pukyong National University, Busan City, Republic of Korea

December 14, 2018



A handwritten signature in black ink, appearing to read 'Minh Thien Tran', is written over the right side of the university logo.

**Minh Thien Tran**

## Contents

Acknowledgements.....	i
Abstract .....	v
List of Figures .....	viii
List of Tables .....	xi
Nomenclature.....	xii
<b>Chapter 1: INTRODUCTION .....</b>	<b>1</b>
<b>1.1 Background and motivation.....</b>	<b>1</b>
1.1.1 Conveyor belt system.....	1
1.1.2 Image processing method of food industry.....	4
<b>1.2 Problem statements.....</b>	<b>6</b>
<b>1.3 Objective and researching method.....</b>	<b>6</b>
<b>1.4 Outline of dissertation and summary of contributions... 8</b>	<b>8</b>
<b>Chapter 2: SYSTEM DESCRIPTION.....</b>	<b>11</b>
<b>2.1 System description.....</b>	<b>11</b>
<b>2.2 Mechanical design .....</b>	<b>12</b>
<b>2.3 Electrical design.....</b>	<b>15</b>
<b>2.4 Configuration of the proposed image processing system .</b> .....	<b>17</b>
<b>2.5 Electronic parts for an image processing system .....</b>	<b>18</b>
<b>Chapter 3: MODELING SYSTEM AND CONTROL DESIGN..</b> .....	<b>19</b>
<b>3.1 System Modeling .....</b>	<b>19</b>

3.2	<b>Model reference adaptive controller design</b> .....	22
3.3	<b>Reference model output signal</b> .....	25
3.4	<b>Simulation results</b> .....	26
3.5	<b>Summary</b> .....	31
<b>Chapter 4: MEASUREMENT OF INJURY RATE ON FISH SKIN BASED ON L*a*b* AND HSV COLOR SPACES</b> .....		32
4.1	<b>Image processing based on L*a*b* color space compared with HSV color space</b> .....	32
4.2	<b>Experiment results</b> .....	37
4.3	<b>Summary</b> .....	41
<b>Chapter 5: DETERMINATION OF INJURY RATE ON FISH SURFACE BASED ON FUZZY C-MEANS CLUSTERING ALGORITHM</b> .....		42
5.1	<b>Proposed injury rate measurement method on fish surface</b> .....	42
5.2	<b>Experiment results</b> .....	48
5.3	<b>Summary</b> .....	53
<b>Chapter 6: CONCLUSIONS AND FUTURE WORKS</b> .....		55
6.1	<b>Conclusions</b> .....	55
6.2	<b>Future works</b> .....	57
<b>REFERENCES</b> .....		58
<b>PUBLICATIONS AND CONFERENCE</b> .....		64
<b>Appendix A: Proof of Eq. (3.15)</b> .....		67



# **Measurement Method of Injury Rate on Fish Skin Using an Image Processing System**

Minh Thien Tran

**Department of Mechanical Design Engineering,  
The Graduate School, Pukyong National University**

## **Abstract**

Nowadays, the conveyor belt system is the most effective method to transport items in factory such as transporting fishes from harbor to factory or transporting fishes on a basement of an image processing system. If the fish is put on the basement of only the image processing system or the conveyor belt system without control, the center position of the fish cannot be matched with the center position of an image processing system. Thus, an effort of designing a conveyor belt system and developing a method measuring injury rate using an image processing algorithm to transport the fishes effectively is very necessary.

To do these tasks for this thesis, the following problems are considered. The first one is to present system description of the fish conveyor belt system to be constructed for this thesis. The second one is to design a control law to control a desired angular position of driving pulley of the fish conveyor system. The third one is to develop an algorithm using image processing method to measure injury rate on fish surface.

Firstly, the full system includes image processing system and a fish conveyor system. A simple dynamic modelling simplifying the fish conveyor system is used for this thesis. However, the dynamic modelling parameters of the system such as viscous friction, rotation friction and break coefficients are considered as unknown variables. The second Newton law is used to obtain the dynamic modeling of a fish conveyor system.

Secondly, a model reference adaptive control (MRAC) law is applied to solve the uncertain parameters of system issue. Two controllers based on the MRAC are described as follows. The sub-controller is to obtain the output signal of a reference model to track a desired angular position of the driving pulley. However, this system is of second order. Therefore, it is difficult to get the stability of the reference model using Lyapunov stability theory. A simple method using the transfer function of the reference model is proposed. The main controller is to obtain the output signal of a real system to track the reference model output signal. The stability of the main controller is surely guaranteed by the Lyapunov stability theory and Babarlat's lemma.

Thirdly, there are several color spaces used in food industry to develop an algorithm using an image processing method.  $L^*a^*b^*$  and HSV color spaces are used generally. Therefore, a direct measurement of injury rate on fish surface compared to  $L^*a^*b^*$  and HSV color spaces is implemented. Based on this comparison, the K-means or Fuzzy C-means clustering algorithm on an image is considered to show clean injury and body shapes of fish. Median, Gaussian and bilateral filters are used to reduce several kinds of noises such as salt and pepper,

random, and Gaussian noise. Moreover, Candy edge detection algorithm is used to detect clearly the boundary between injuries and body fish on color spaces. Furthermore, the Fuzzy C-means clustering algorithm is applied to solve overlapped data issue at the boundary between injury and fish body and measure the injury rate on fish skin more exactly.

Finally, the experiments are done on fishes to test the proposed image processing algorithms. The real data of the injury fish is measured by Photoshop software and compared with the experimental results of the proposed image processing method. Simulation and experimental results are shown to verify the effectiveness and performance of the proposed controller and the proposed image processing algorithm.

**Keywords:** MRAC, Transfer function, Mapping method, Belt conveyor system, L\*a\*b\* color space, Fuzzy C-means clustering.

## List of Figures

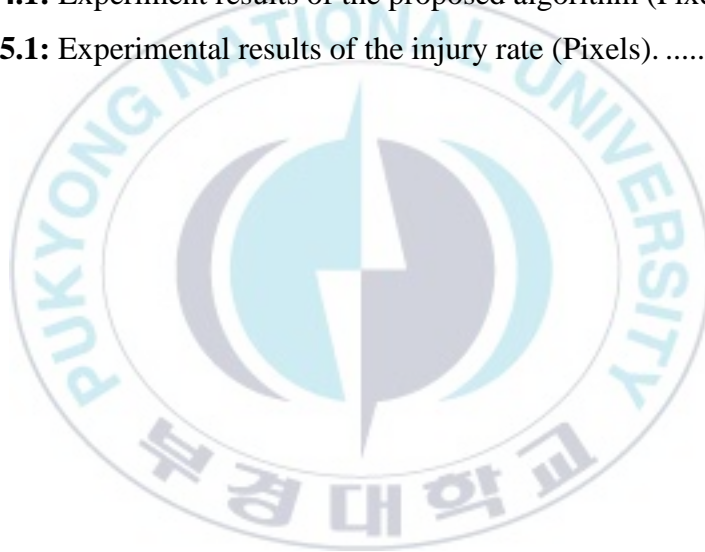
Fig. 1.1 A conveyor system at a plant.....	1
Fig. 1.2 Conveyor belt systems.....	2
Fig. 2.1 Fish conveyor fish line at Pelagic factory .....	11
Fig. 2.2 Mechanical conveyor system – front side .....	12
Fig. 2.3 Mechanical conveyor system – back side.....	13
Fig. 2.4 Mechanical conveyor system – inside .....	13
Fig. 2.5 Detailed mechanical fish conveyor belt system .....	14
Fig. 2.6 Electrical design flowchart .....	16
Fig. 2.7 Frequency inverter .....	16
Fig. 2.8 Configuration of a computer vision system for image processing .....	17
Fig. 3.1 Configuration of for simplified modeling of the fish conveyor belt system.....	19
Fig. 3.2 Desired angular position of the fish conveyor belt system.	23
Fig. 3.3 Block diagram of the proposed MRAC scheme .....	26
Fig. 3.4 Output angular position of MRAC control.....	28
Fig. 3.5 Tracking error and modeling error .....	29
Fig. 3.6 Voltage control input signal .....	30
Fig. 3.7 Ideal gains for update control law .....	30
Fig. 3.8 Angular velocity .....	31
Fig. 4.1 L*a*b* color space .....	32
Fig. 4.2 HSV color space .....	34
Fig. 4.3 Image processing algorithm for L*a*b* color space and HSV color space .....	34
Fig. 4.4 Original color image.....	37

Fig. 4.5 L*a*b* color space image .....	37
Fig. 4.6 HSV color space image .....	38
Fig. 4.7 Original channel “a” image on L*a*b* color space .....	38
Fig. 4.8 New channel “a” image on L*a*b* color space.....	38
Fig. 4.9 Binary image fish shape on L*a*b* color space .....	38
Fig. 4.10 Binary injury image on L*a*b* color space.....	38
Fig. 4.11 Binary injury image on HSV color space before morphological processing .....	39
Fig. 4.12 Binary image fish shape on HSV color space .....	39
Fig. 4.13 Binary injury image on HSV color space after morphological processing .....	39
Fig. 4.14 Edge detection injuries and shape on fish image on HSV color space .....	39
Fig. 4.15 Edge detection injuries and shape on fish image on L*a*b* color space .....	39
Fig. 5.1 Flowchart of the proposed image processing method .....	46
Fig. 5.2 Cropped image from ZED stereo camera of sample 1 filtered by Median and Bilateral filter .....	48
Fig. 5.3 Fuzzy C-means clustering algorithm combined with L*a*b* color space image of sample 1 .....	48
Fig. 5.4 Original channel “a” image of sample 1 .....	49
Fig. 5.5 New channel “a” image of sample 1 .....	49
Fig. 5.6 Binary injury image of sample 1 filtered by Median filter.	49
Fig. 5.7 Channel “b” image of sample 1 filtered by Gaussian filter	49
Fig. 5.8 Binary body image of sample 1 .....	49
Fig. 5.9 Binary body image of sample 1 filtered by Median filter ..	49
Fig. 5.10 Cropped image from ZED stereo camera of sample 2 filtered by Median and Bilateral filter .....	50

Fig. 5.11 Fuzzy C-means clustering algorithm combined with L*a*b* color space image of sample 2.....	50
Fig. 5.12 Original channel “a” image of sample 2.....	50
Fig. 5.13 New channel “a” image of sample 2 .....	50
Fig. 5.14 Binary injury image of sample 2 filtered by Median filter.....	50
Fig. 5.15 Channel “b” image of sample 2.....	51
Fig. 5.16 Channel “b” image of sample 2 filtered .....	51
Fig. 5.17 Binary body image of sample 2.....	51
Fig. 5.18 Binary body image of sample 2 after filtered by Median filter.....	51
Fig. 5.19 K-means clustering algorithm combined with L*a*b* color space image of sample 1 .....	51
Fig. 5.20 Binary injury image of sample 1 filtered by Median filter (K-means) .....	52
Fig. 5.21 Binary body image of sample 1 filtered by Median filter (K-means) .....	52
Fig. 5.22 K-means clustering algorithm combined with L*a*b* color space image of sample 2.....	52
Fig. 5.23 Binary injury image of sample 2 filtered by Median filter (K-means) .....	52
Fig. 5.24 Binary body image of sample 2 filtered by Median filter (K-means) .....	52

## List of Tables

<b>Table 2.1:</b> Specification of the mechanical fish conveyor belt system design .....	15
<b>Table 2.2:</b> Encoder parameters.....	16
<b>Table 2.3:</b> Frequency inverter parameters[34].....	17
<b>Table 2.4</b> Specification of electronic parts for the proposed image processing system used in this thesis .....	18
<b>Table 4.1:</b> Experiment results of the proposed algorithm (Pixels) ..	40
<b>Table 5.1:</b> Experimental results of the injury rate (Pixels). .....	53





## Nomenclature

<b>Items</b>	<b>Description</b>	<b>Unit</b>
$J_1, J_2$	Moment of inertia of the drive pulley and the driven pulley	kgm <sup>2</sup>
$D_1, D_2$	Diameters of moment of inertia of the drive pulley and the driven pulley	m
$M_1, M_2$	Mass of moment of inertia of the drive pulley and the driven pulley	kg
$k$	Amplifier gain	J/V
$u$	VDC voltage input signal	V
$e$	Modeling error	rad, rad/s
$e_m$	Tracking error	rad
$R_N$	Normal reaction force	N
$A$	Dynamic parameter matrix of fish conveyor belt	-
$b$	Input vector of fish conveyor belt	-
$c$	Output vector of fish conveyor belt	-
$x$	Modeling state variable of fish conveyor belt	rad, rad/s
$y$	Output angular position of fish conveyor belt	rad
$A_m$	Dynamic parameter matrix of the reference model	-
$b_m$	Input vector of the reference model	-
$x_m$	Modeling state variable of the reference model	rad, rad/s



$y_m$	Output angular position of the reference model	rad
$P$	Positive definite matrix belonging to fish conveyor belt	-
$Q$	Positive definite matrix belonging to fish conveyor belt	-
$G_m$	Transfer function	-
$a_0$	Bound constant value	-
$t_{r1}, t_{r2}$	Starting time and ending time	s
$L^*$	Luminance	-
$a^*, b^*$	Chromaticity layer	-
$a_{new}(x,y)$	Output pixel of adjusting algorithm	-
$a(x,y)$	Input pixel of adjusting algorithm	-
$h$	Coefficient conditional environment	-
$x,y$	Coordinate of pixels	-
$G_0(x,y)$	Gaussian filter	-
$w$	Neighborhood defined by user	-
$a[i,j]$	Neighborhood of elements	-
$i,j$	Local coordinate	-
$b[x,y]$	Center location of the image	-
$g(i,j)$	Output pixel's value	-
$f(i+m,j+l)$	Input pixel value	-
$f(i,j)$	Input pixel value	-
$h(m,l)$	Coefficient of filter	-
$m,l$	Position in image	-
$J_p$	Objective function to be minimized.	-
$J$	Objective function to be minimized.	-
$D$	Number of data point	-

$N$	Number of clusters	-
$n$	Data points	-
$z$	Cluster membership value	-
$p$	Fuzzy partition matrix, $m>1$	-
$c_j$	Center of the $j^{\text{th}}$ cluster	-
$\theta_1, \theta_2$	Angular position of the drive pulley and the driven pulley	rad
$\theta_{ref}$	Desired angular position of the drive pulley and the driven pulley	rad
$\theta_d$	Reconstructed reference signal	rad
$\theta_c$	Bound constant value	rad
$\xi_1$	Viscous friction coefficients of the drive pulley	Js/rad
$\xi_2$	Viscous friction coefficients of the driven pulley	Js/rad
$\xi$	Viscous friction coefficients	Js/rad
$\rho_1$	Rotation friction coefficients of the drive pulley	m/rad
$\rho_2$	Rotation friction coefficients of the driven pulley	m/rad
$\rho_i$	Rotation friction coefficients	m/rad
$\tau_1, \tau_2$	Sufficient torques	J
$\hat{k}_x$	Estimated parameters of the unknown ideal gain	V/rad, Vs/rad
$\hat{k}_r$	Estimated parameters of the unknown ideal gain	V/rad
$\omega_n$	Undamped natural frequency	rad/s

$\zeta$	Damping ratio	-
$\mu_x, \mu_y$	Means	-
$\sigma_x, \sigma_y$	Represent variances	-
$\mu_{ij}$	Degree of membership	-
$\alpha, \beta$	Gain and bias parameters, $\alpha, \beta > 0$	-
$\gamma_1$	Adaption learning gain, $\gamma_1 > 0$	-
$\gamma_2$	Adaption learning gain, $\gamma_2 > 0$	-



**1.1 Background and motivation****1.1.1 Conveyor belt system**

A conveyor system is a common piece of mechanical handling equipment that moves materials from one location to another in industries. It allows a quick and efficient transportation equipment of materials for a wide variety in industries. These conveyor systems are commonly used in postal sorting offices and airport baggage handling systems as shown in Fig. 1.1.



Fig. 1.1 A conveyor system at a plant

A belt conveyor system is one of several types of the conveyor system. A belt conveyor system consists of two or more pulleys with an endless loop of handling equipments. The powered pulley is called the drive pulley, while the unpowered pulley is called the idle pulley or driven pulley. Nowadays, belt conveyors are the most commonly used powered conveyors because they are the most flexible and cheap.

The large product or small product can be moved directly on the belt as shown in Fig. 1.2.



Fig. 1.2 Conveyor belt systems

In fact, the conveyor belt system is the most effective method to transport goods or items. Therefore, controlling the conveyor belt system to improve effective transportation of items is very necessary. Until now, there are three method of operating the conveyor belt system: manual, semi-automatic and automatic operation.

For last decades, there have been great of efforts to design and control position and velocity using adaptive control law to control angular velocity of the induction conveyor line, etc. M. C. Tai et al. [1] designed and experimented to control a working table to track position of a work-piece on a moving conveyor belt. A servo controller design method for velocity control of a fish sorting conveyor system using a polynomial differential operator was presented by T. H. Nguyen et al. [2]. The induction conveyor line was developed by H. H. Nguyen, which used adaptive control law to control angular velocity of the induction conveyor line with saturation input, robust adaptation and

bounded disturbance [3]. A. A. A. El-Gammal et al. [4] modified PID controller for DC motor drives using a PSO method, which gave the minimum integral absolute error between the velocity demand and the reference response. All of the typical controllers strictly require a system with known parameters due to modeling design, which are only control angular velocity.

A modeling of the fishing conveyor system has uncertain parameters such as a viscous friction and friction factor between pulley and belt, moments of inertia of the pulleys, pulling force, etc. to be exactly unmeasured [2, 3]. Adaptive control is developed to control both linear and nonlinear dynamical systems with uncertain variables. The stability and robustness issue of adaptive control with uncertain variables were documented in several literatures [5, 6].

A model reference adaptive control (MRAC) method was constructed on Lyapunov stability theory which was necessary to show the stability of system and further conditions in an adaptive control field such as [7, 8]. The MRAC method includes direct MRAC, indirect MRAC, MRAC with input linear saturation and modified MRAC (MMRAC), etc [9-11]. In this case, to improve the tracking performance, the adaption learning gain value should be chosen by trial and error method. However, most of the methods mentioned above frequently used for the first order system with unknown parameters. In complicated case, A. Das et al. [12] studied cooperative adaptive control and neural network for synchronization of the second order systems with unknown nonlinearities. This method also was based on Lyapunov stability theory under the condition of boundedness of the tracking error.

Today, there are several problems to consider uncertain parameters, second order systems and complicated control law design. Therefore, a simple angular position controller for a second order fish conveyor belt system with uncertain parameters using the MRAC method needs to be considered.

### 1.1.2 Image processing method of food industry

Computer vision is the science that aims to a similar capability of the human eyes to the machine or computer. Useful information is extracted from the images using the computer vision. It involves the development of an image processing algorithm based on each application.

From the early 20<sup>th</sup> century, the computer vision technology is widely implemented in the industry fields, specially the food industry field. N. A. Valous et al. [13] described clearly application of computer vision technology in the food and beverage industries. Specially, color image segmentation is important in computer vision, which was reviewed by D. J. Bora et al. [14, 15]. Therefore, color image segmentation proposed the new approach which applied an image processing method in food industry to be easier and more effective. Using color image segmentation method in food industry, S. Dhameliya et al. [16] applied an image processing method to estimate volume of mango. A novel measurement of species and length of fish using an image segmentation processing method was proposed by D. J. White et al. [17]. Thus, the image processing method is an method to acts as the human eye in the role of monitoring and estimating the quality of objects.



However, there are several color spaces used in image segmentation processing. Generally in food industry, L\*a\*b\*, HSV and RGB color spaces have been widely used for pre-processing step in image segmentation processing [18, 19]. Therefore, using and choosing a right color space is a crucial issue in an image segmentation processing algorithm. I. L. Waetherall et al. [20] measured skin color of healthy volunteers using L\*a\*b\* color space. To be more clear, K. Leon et al. [21] showed a computational solution to allow digital images in L\*a\*b\* color units for each pixel of the digital RGB image. Moreover, they presented 5 models such as online, quadratic, gamma, direct and neural network to convert RGB color space into L\*a\*b\* color space for evaluating appearance and color of food. Color measurement of food product [22] using L\*a\*b\* and RGB color space, development of image segmentation using L\*a\*b\* color space based on a genetic algorithm [23], correlation between L\*a\*b\* color space and Carotenoid Content in pumpkins and squashes [24] and evaluation of color behavior during ripening of mango using L\*a\*b\* color space [25] were proposed.

In order to carry out an image segmentation analysis in food, it is necessary to know the color of pixels on the surface of the food items. The most color space used for measuring color in food is the L\*a\*b\* color space of color spaces because it has uniform distribution and is very close to human perception of color. Therefore, developing a new algorithm for measuring injury rate on fish surface based on L\*a\*b\* color space is also necessary.



## 1.2 Problem statements

The problem statements to design and control a fish conveyor belt system and to develop a method measuring injury rate of fishes using an image processing method are described as follows:

- To design and manufacture a fish conveyor belt system and an image processing system.
- To describe a modeling of the fish conveyor belt system and to design an angular position controller for the fish conveyor belt system with unknown parameters and the second order dynamic equation.
- To choose a color space to be the most suitable for fish application.
- To solve overlapped data between injury shape and fish body.

## 1.3 Objective and researching method

The objective of this thesis is controlling an angular position of a fish conveyor belt system for determining injury rate on fish surface using an image processing method.

For controller system issue, system modeling is needed to analyze the mechanical and electric behaviors. A simple model modeling is obtained based on the mechanical design. However, the essential parameters of the simple modelling system are uncertain variables. To solve this issue, a model reference adaptive control (MRAC) approach is used for designing a control law without knowing system parameters. To design an angular position controller for a fish belt conveyor system,

the followings are done. Firstly, a reference model is chosen such that the angular position output of the reference model tracks a given desired reference input using a mapping method [26, 27]. Secondly, the angular position output of the system tracks the angular position output of the reference model by using MRAC law.

For image processing issue, system design and a new image processing algorithm are proposed to improve accuracy of injury rate on fish surface. To do this issue, image segmentation of fish is needed. However, in food industry,  $L^*a^*b^*$ , HSV and RGB color spaces are widely used for image segmentation processing. To solve this problem, the followings step are done. Firstly, a measurement method of injury rate on fish surface and performance comparison of image segmentation based on  $L^*a^*b^*$  and HSV color spaces are proposed to be sure that  $L^*a^*b^*$  color space is better than other color space in this application. Secondly, the clustering, analysis and extraction of useful information from a single image or a sequence of images are performed to separate more clearly injury and body shapes of fish using the K-means, Fuzzy C-means, Expectation Maximization (EM) and Hierarchical clustering algorithms[28-33]. Thirdly, there are several noises in an image such as salt and pepper, random, white, shot and Gaussian noises. All of these noises give false information of injury and body shapes of fish. Therefore, Median, Gaussian, Bilateral and morphological filters give a solution to solve the noise problem. Fourthly, the determination of injury rate on fish surface based on Fuzzy C-means clustering algorithm is proposed to solve overlapped data issue. Finally, the experiments are done on fishes to test the above proposed image processing algorithms. The real data of the injury fish

is measured by Photoshop software and compared with the experimental results of the proposed image processing method. Simulation and experimental results are shown to verify the effectiveness and performance of the proposed controller and the proposed image processing algorithm.

#### **1.4 Outline of dissertation and summary of contributions**

##### **➤ Chapter 1: Introduction**

Background and motivation, problem statements, objective and researching methods and the outline and summary of contributions of this thesis are presented.

##### **➤ Chapter 2: System description**

This chapter shows the structure of a fish conveyor belt system and an image processing system used for this thesis. The conveyor system includes: drive and driven pulley, conveyor belt system, motor, motor base and bearing. The mechanical and electric system are designed and manufactured.

The image processing system includes computer, USB 3.0 Hub and image processing box (camera, lamps, image processing frame). Moreover, the USB 3.0 Hub connects ZED stereo camera with the computer, which is supported by its power with 12VDC.

➤ **Chapter 3: Modeling system and control design**

A simple modeling of the fish conveyor belt system is presented to design an angular position controller. A dynamic modeling of the fish conveyor belt system is introduced based on the second Newton law.

An angular position controller design method using MRAC for the fish conveyor belt system with uncertain parameters is proposed. The stability of the MRAC controller is surely guaranteed by the Lyapunov stability theory and Babarlat's lemma.

➤ **Chapter 4: Measurement of injury rate on fish skin and performance comparison based on L\*a\*b\* and HSV color spaces**

L\*a\*b\* and HSV color spaces are import step in image segmentation. Choosing a right color space is crucial issue for image processing method. To do these works, HSV color space or L\*a\*b\* color space is chosen in the image processing method. This chapter chooses a right color space for measurement of injury rate on fish surface by comparison to real data. A method to adjust a value of channel “a\*” to realize injury on fish surface clearly is proposed. Moreover, Candy edge detection algorithm is used to detect clearly the boundary between injuries and body of a fish on color spaces. Therefore,

L\*a\*b\* color space and HSV color space in measuring the injury rate are compared.

➤ **Chapter 5: Determination of injury rate on fish surface based on Fuzzy C-means clustering algorithm**

There are overlapped data between injury shape and fish body. To solve the overlapped data problem, the determination of injury rate on fish surface based on a Fuzzy C-means clustering algorithm is proposed. Moreover, median, Gaussian and bilateral filters are used to reduce several kinds of noises such as salt and pepper, random, and Gaussian noise. Therefore, the results of the Fuzzy C-means clustering algorithm, the K-means clustering algorithm and the real data in measuring the injury rate are compared.

➤ **Chapter 6: Conclusions and future works**

Conclusions for this dissertation and future ideas for future work are illustrated.

**2.1 System description**

Today, fish is very important food product for keeping human life. Therefore, maintaining the quality of fish is needed from harvest to consumption. Careful handling of fish on ship to the processing plant is performed to maintain the high quality of the product. The fishes are pumped from ship to a received area on land by a fishing pump. At cleaning area, the dirt and blood of fish are removed from fish. The fishes are sorted by size of fish one by one using a sorter such as an image processing conveyor belt system to select and remove injured fishes. Finally, the fishes move to packing area to pack and freeze.

Fig. 2.1 shows the structure of fish conveyor fish line modules for fish process at an industrial factory.



Fig. 2.1 Fish conveyor fish line at Pelagic factory



## 2.2 Mechanical design

Selecting injured fishes manually is hard work with low efficiency. So, an online selecting method is needed. To do this work, an image processing method is usually considered. However, an image processing method and a good mechanical system design are needed. The mechanical system is designed as shown in Fig. 2.2.

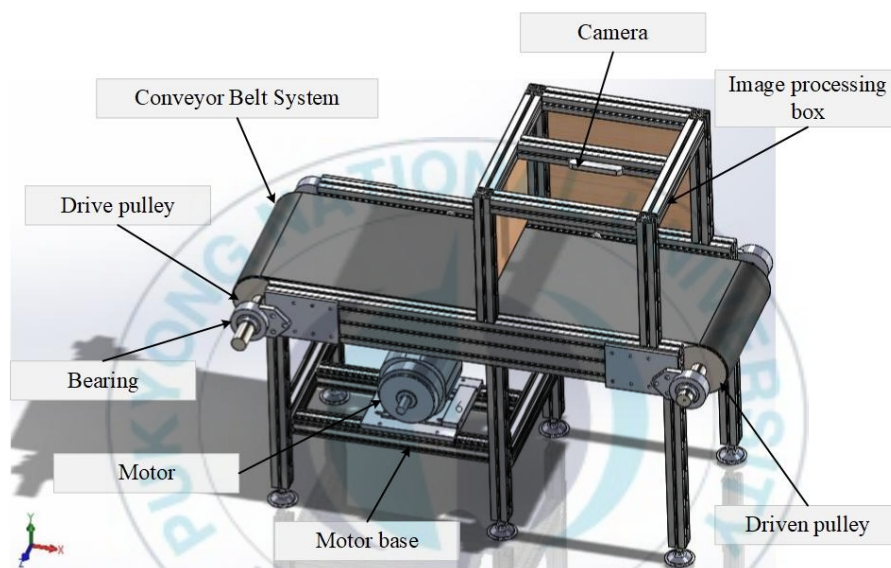


Fig. 2.2 Mechanical conveyor system – front side

Fig. 2.2 shows the mechanical conveyor system from front side. The system consists of two main parts: conveyor system and image processing box system. The conveyor system includes: drive and driven pulley, conveyor belt system, motor, motor base and bearing. The image processing system includes: image processing box, camera, cover and aluminum frames.

Fig. 2.3 shows the back side of the mechanical conveyor system. In the back side of the mechanical conveyor, system mechanical design and image processing box with covers are shown clearly. However, some covers are hid in the inside frame of the image processing box.

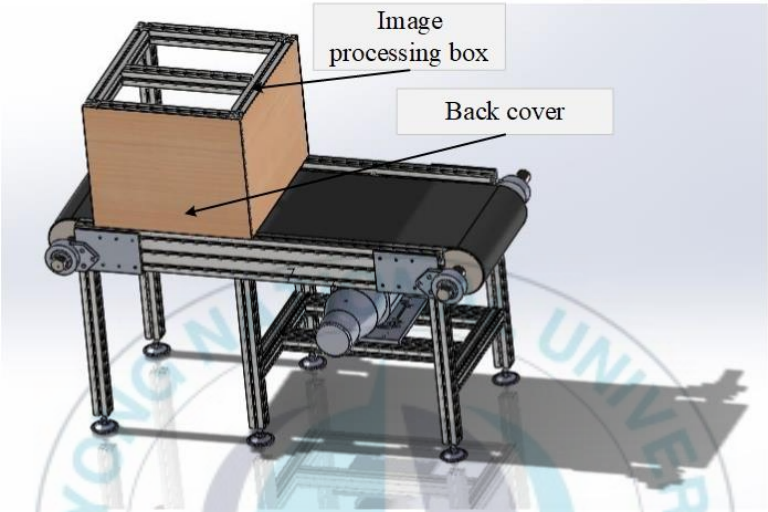


Fig. 2.3 Mechanical conveyor system – back side

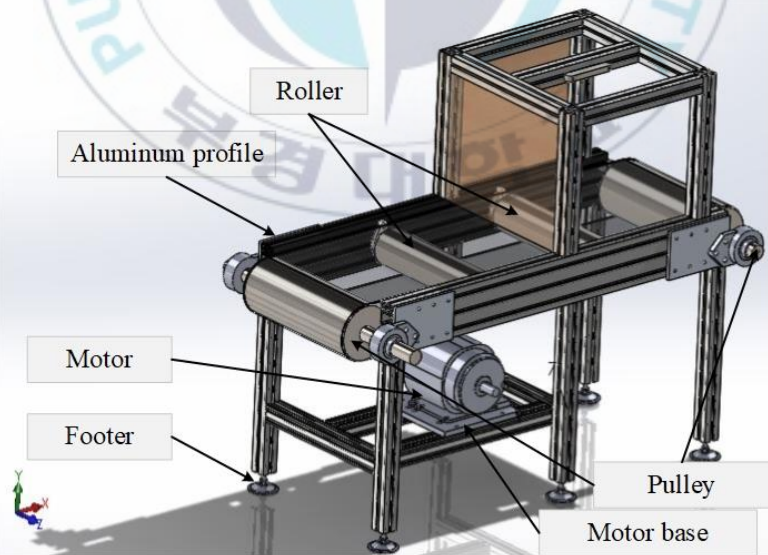


Fig. 2.4 Mechanical conveyor system – inside



Fig. 2.5 show the inside structure of the fish conveyor belt system. Inside the conveyor belt, two more rollers are installed to create tension force for the conveyor belt. One motor base, one conveyor belt and aluminum profile to ensure rigidity for all system are installed.

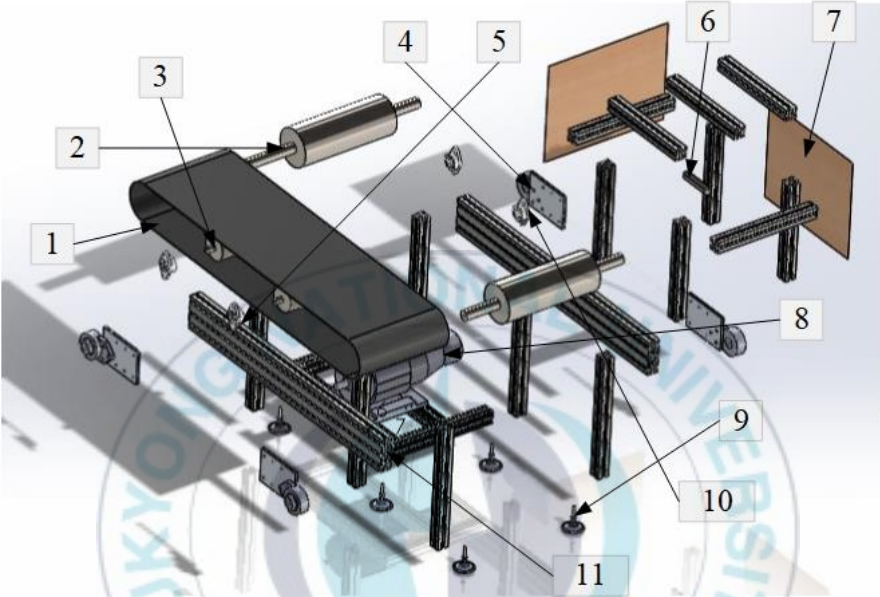


Fig. 2.5 Detailed mechanical fish conveyor belt system

Fig. 2.5 shows a detailed mechanical fish conveyor belt system and the specification of the mechanical fish conveyor belt system is shown on Table 2.1.

No.	Name	Description	Quantity
1	Belt	Color: black	1
2	Pulley	Diameter: 150cm	2
3	Roller	Diameter: 100cm	2
4	Pulley bearing	SKF bearing	4
5	Roller bearing	SKF bearing	4
6	Camera	ZED stereo camera	1

7	Cover		5
8	Motor	AC motor	1
9	Footer		6
10	Lamp	LED, 8W – 220V	4
11	Aluminum profile	30x30 mm	--

**Table 2.1:** Specification of the mechanical fish conveyor belt system design

### 2.3 Electrical design

Fig. 2.6 shows the flowchart for controlling angular position of the fish conveyor belt system. The microcontroller part sends control input signals to frequency inverter and receives sensor signal of encoder to track reference profiles. The encoder is attached on drive pulley to detect the practical angular position and sends it to microcontroller (Arduino microcontroller). Frequency inverter receives control input signal DC voltages (0-5V) from Arduino microcontroller. Based on control input signal DC voltages (0-5V), the frequency inverter controls the power supply for AC motor. The drive pulley of the fish conveyor belt system is driven by toothed belt from motor rotation. The specifications of the encoder and the frequency inverter are shown in Table 2.2 and Table 2.3.

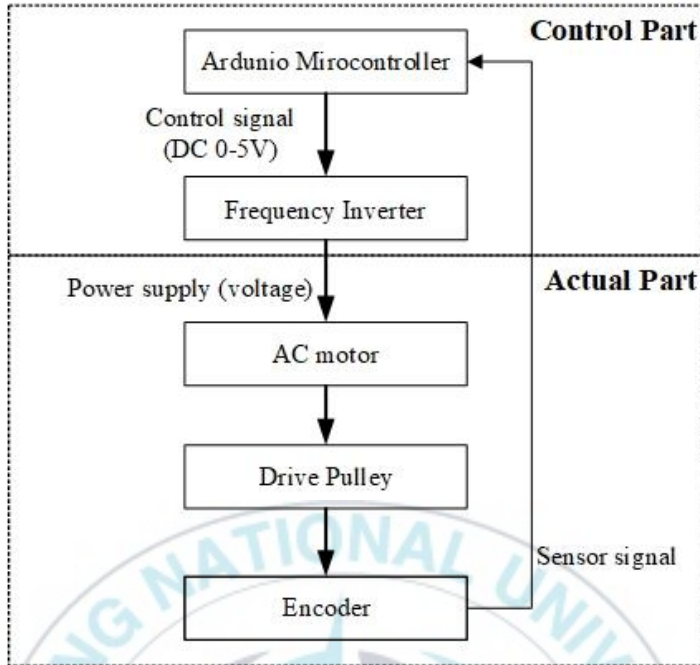


Fig. 2.6 Electrical design flowchart

Table 2.2: Encoder parameters

Parameter	Value
Power supply	5-30 V DC
Type	Hollow
Pulse rate	1024 ppr
Type of connection	Radial cable



Fig. 2.7 Frequency inverter

**Table 2.3:** Frequency inverter parameters[34]

Parameter	Value
Power supply	5-30 VDC
Output voltage	Three-phase 200-240V
Input voltage	200-240V (50Hz/60Hz)
Control method	V/F, PID
Fre. Control rage	0.1-400Hz
Analog input	0-12V
Motor capacity	0.1 – 15KW

## 2.4 Configuration of the proposed image processing system

The image processing system includes computer, USB 3.0 Hub and image processing box, ZED stereo camera, lamps, cloth cover basement and image processing algorithm. A computer vision system for image processing to calculate the injury rate of fish is constructed as illustrated in Fig. 2.8.

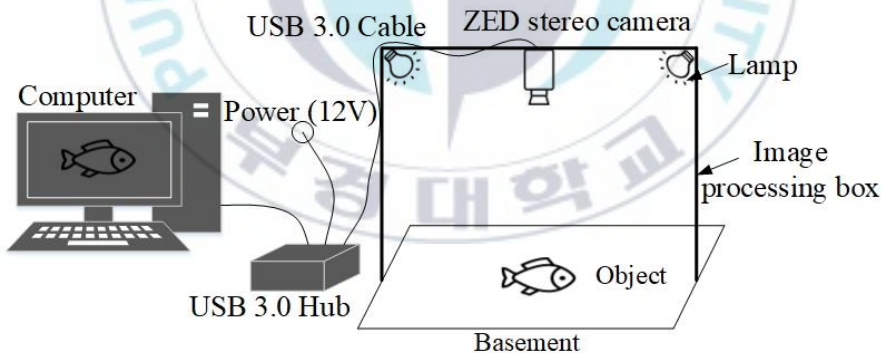


Fig. 2.8 Configuration of a computer vision system for image processing

The ZED stereo camera has to be perpendicular to basement to capture the good quality image and avoid the scattering of light from the lamps [35]. Basement is designed as green color to improve accuracy of a proposed image processing algorithm based on L\*a\*b\* color space because green color is opposite of the red of the wound on fish.

Moreover, the USB 3.0 Hub connects ZED stereo camera with the computer, which is supported by its power with 12VDC. Therefore, the image obtained using the USB 3.0 Hub's power has better quality than that obtained without using the USB 3.0 Hub's power. The basement and the ZED stereo camera also have to be covered by clothes to avoid the effect of the light from external environment.

## 2.5 Electronic parts for an image processing system

The specification of the electronic parts for the proposed image processing system used in this thesis is shown on Table 2.4.

**Table 2.4** Specification of electronic parts for the proposed image processing system used in this thesis

Parameter	Value
Mini PC	Core i7, RAM 8GB
USB Hub	12VDC
ZED stereo camera	Mode (2.2K, 1080p, 720p, WVGA)
LED lamp	8W – 220V

## Chapter 3: MODELING SYSTEM AND CONTROL DESIGN

### 3.1 System Modeling

Configuration for the simplified model of the fish conveyor belt system is shown in Fig. 3.1. In Fig. 3.1,  $J_1$  and  $J_2$  are moments of inertia of the drive pulley and the driven pulley;  $\theta_1$  and  $\theta_2$  are the angular position of the drive pulley and the driven pulley;  $\xi_1$  and  $\xi_2$  are viscous friction coefficients of bearing the drive pulley and the driven pulley;  $\rho_1$  and  $\rho_1$  are rotation friction coefficients between pulley and belt;  $D_1$  and  $D_2$  are diameters of the drive pulley and the driven pulley, respectively.

The frequency inverter with VDC voltage input signal controls the AC motor to create sufficiently torque which drives the part of the fish conveyor belt system shown in Fig. 3.1.

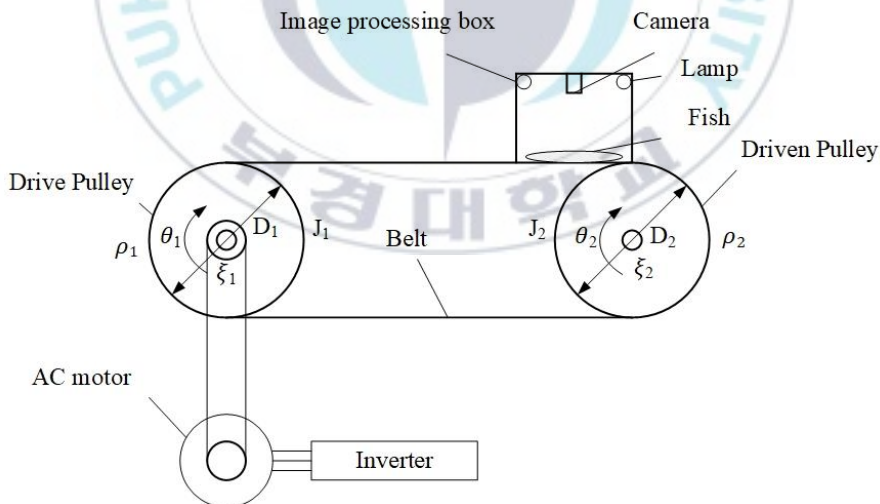


Fig. 3.1 Configuration of for simplified modeling of the fish conveyor belt system

To simplify the fishing conveyor modeling, the following assumptions are given:

- Coupling is rigid and short.
- Belt's slippage on the pulleys is negligible.
- Belt elasticity is also negligible to camera.
- Fish on belt is also in right position to camera.
- Driving has no loss in efficiency.

Since both the drive pulley and the driven pulley are assumed to be a type of solid cylinder, their moments of inertia are given as follows:

$$\begin{cases} J_1 = \frac{1}{8} m_1 D_1^2 \\ J_2 = \frac{1}{8} m_2 D_2^2 \end{cases} \quad (3.1)$$

where  $m_1$  and  $m_2$  are masses of the drive pulley and the driven pulley of the fish conveyor, respectively.

By applying the Newton's second law to rotational pulleys, viscous friction and rotation friction, sufficient torques for the drive pulley and the driven pulley of the fish conveyor belt system are given as follows [3, 36]:

$$\begin{cases} \tau_1 = J_1 \ddot{\theta}_1 + \xi_1 \dot{\theta}_1 + \rho_1 R_N \theta_1 \\ \tau_2 = J_2 \ddot{\theta}_2 + \xi_2 \dot{\theta}_2 + \rho_2 R_N \theta_2 \end{cases} \quad (3.2)$$

where  $\tau_1$  and  $\tau_2$  are torques sufficient for the drive pulley and the driven pulley of the fish conveyor belt system.  $\rho_i R_N \theta_i$  is rotation friction torque between belt and pulley [36].  $R_{Ni}$  is normal reaction



force between belt and pulley.  $\rho_i$  are rotation friction coefficients between pulley and belt.

Under the above assumptions, the sufficient torque to drive the driven pulley of the fish conveyor belt system can be expressed as follows:

$$\tau = \tau_1 + \tau_2 = J\ddot{\theta}_1 + \xi\dot{\theta}_1 + \rho R_N \theta_1 \quad (3.3)$$

where  $J = J_1 + J_2$ ,  $\xi = \xi_1 + \xi_2$ ,  $\rho = \rho_1 + \rho_2$ .  $\tau$  is a sufficient torque to drive the fish conveyor belt system given as follows:

$$\tau = ku \quad (3.4)$$

where  $k$  is an amplifier gain, and  $u$  is VDC voltage input signal of the frequency inverter to create the desired torque.

By using a state-space method, dynamics of angular position of the conveyor based on Eqs. (3.3) ~ (3.4) can be expressed as a SISO system in the state space as follows:

$$\begin{cases} \dot{\mathbf{x}} = \mathbf{A}\mathbf{x} + \mathbf{b}u \\ y = \mathbf{c}\mathbf{x} \end{cases} \quad (3.5)$$

where  $\mathbf{x} = [x_1 \ x_2]^T = [\theta \ \dot{\theta}]^T$  are system state vector of the fish conveyor belt system.  $y = \theta$  is an output angular position value of the fish conveyor belt system measured by encoder on the drive pulley.  $u$  is control input signal.  $\mathbf{A}$  and  $\mathbf{b}$  are unknown constant parameter matrix and control distribution vector given as follows:

$$\mathbf{A} = \begin{bmatrix} 0 & 1 \\ a_{21} & a_{22} \end{bmatrix}, \mathbf{b} = \begin{bmatrix} 0 \\ b_{21} \end{bmatrix}, \mathbf{c} = [1 \ 0]$$



where  $a_{21} = \frac{-\rho R_N}{J}$ ,  $a_{22} = \frac{-\xi}{J}$  and  $b_{21} = \frac{k}{J}$

### 3.2 Model reference adaptive controller design

The reference input of the fish conveyor belt system is composed of a ramp function input and a step function input. The model reference system of the fish conveyor belt system of Eq. (3.5) used for this thesis is chosen by:

$$\begin{cases} \dot{\mathbf{x}}_m = \mathbf{A}_m \mathbf{x}_m + \mathbf{b}_m \theta_{ref} \\ y_m = \mathbf{c} \mathbf{x}_m \end{cases} \quad (3.6)$$

where  $x_m = [x_{1m} \ x_{2m}]^T = [\theta_m \ \dot{\theta}_m]^T$  is the model reference system state vector,  $y_m = \theta_m$  is the output of the reference model system.  $\theta_{ref}$  is the desired angular position of the fish conveyor belt system shown in Eq. (3.7) and Fig. 3.2:

$$\theta_{ref} = \begin{cases} a_0 t & \text{if } 0 \leq t \leq t_{r1} \\ \theta_c & \text{if } t_{r1} \leq t \leq t_{r2} \end{cases} \quad (3.7)$$

where  $\theta_c$  and  $a_0$  are bound constant values,  $t_{r1}$  and  $t_{r2}$  are the ending times of changing time and ending time for one controlling circle, respectively. The controlling circle is the reference ( $\theta_{ref}$ ) from starting time 0s to ending time  $t_{r2}$ .

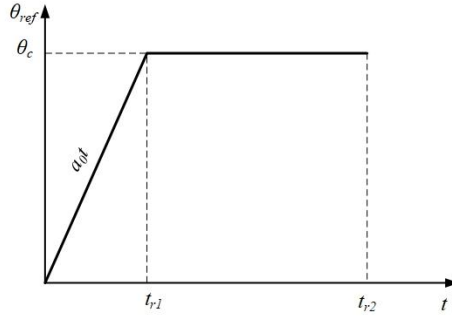


Fig. 3.2 Desired angular position of the fish conveyor belt system

The model reference adaptive controller for position control based on the following assumption:

- Given a known Hurwitz matrix  $A_m \in \mathbb{R}^{2 \times 2}$  and known vector  $\mathbf{b}_m$ , there exists an unknown ideal gain vector  $\mathbf{k}_x \in \mathbb{R}^{1 \times 2}$  and an unknown ideal gain constant  $k_r$  satisfying the following:

$$\begin{cases} \mathbf{A} + \mathbf{b}\mathbf{k}_x = \mathbf{A}_m \\ \mathbf{b}k_r = \mathbf{b}_m \end{cases} \quad (3.8)$$

A control input law is designed as follows:

$$u = \hat{\mathbf{k}}_x \mathbf{x} + \hat{k}_r \theta_{ref} \quad (3.9)$$

where  $\hat{\mathbf{k}}_x, \hat{k}_r$  are the estimated parameters of the unknown ideal gains  $\mathbf{k}_x$  and  $k_r$ . The estimated parameters are updated online by the following adaptive laws in Theorem 3.1.

A tracking error between the output of the reference model system and the desired angular position of the fish conveyor belt system is defined as:

$$e_m = y_m - \theta_{ref}$$

A modeling error vector  $\mathbf{e} = [e_1 \ e_2]^T$  between the system state vector and the model reference system state vector is defined as:

$$\mathbf{e} = \mathbf{x} - \mathbf{x}_m \quad (3.10)$$

Subtracting Eq. (3.5) from Eq. (3.6) and combining Eq. (3.8) and Eq. (3.9) leads to the following:

$$\begin{aligned} \dot{\mathbf{e}} &= \dot{\mathbf{x}} - \dot{\mathbf{x}}_m = \mathbf{A}\mathbf{x} + \mathbf{b}u - \mathbf{A}_m\mathbf{x}_m - \mathbf{b}_m\theta_{ref} \\ &= \mathbf{A}_m(\mathbf{x} - \mathbf{x}_m) + \mathbf{A}\mathbf{x} + \mathbf{b}\hat{\mathbf{k}}_x^T\mathbf{x} - \mathbf{A}_m\mathbf{x} - \mathbf{b}_m\theta_{ref} + \mathbf{b}\hat{k}_r\theta_{ref} \\ \dot{\mathbf{e}} &= \mathbf{A}_m\mathbf{e} + \mathbf{b}(\Delta\mathbf{k}_x\mathbf{x} + \Delta k_r\theta_{ref}) \end{aligned} \quad (3.11)$$

where  $\Delta\mathbf{k}_x = \hat{\mathbf{k}}_x - \mathbf{k}_x, \Delta k_r = \hat{k}_r - k_r$

**Theorem 3.1** A model reference adaptive control system is defined by Eq. (3.5) and Eq. (3.6) is stable provided that the system control input in Eq. (3.8) and adaption update laws are given as:

$$\dot{\hat{\mathbf{k}}}_x^T = -\gamma_1 \mathbf{e}^T \mathbf{P} \mathbf{b} \mathbf{x}, \quad \dot{\hat{k}}_r = -\gamma_2 \mathbf{e}^T \mathbf{P} \mathbf{b} \theta_{ref} \quad (3.12)$$

where  $\hat{\mathbf{k}}_x, \hat{k}_r$  are estimated parameters and  $\gamma_1, \gamma_2$  are positive adaption learning gain value.

**Proof of theorem 3.1** To demonstrate the stability of the control laws, the Lyapunov function candidate is chosen as follows:

$$V = \mathbf{e}^T \mathbf{P} \mathbf{e} + \frac{1}{\gamma_1} \Delta\mathbf{k}_x^T \Delta\mathbf{k}_x + \frac{1}{\gamma_2} k_r^2 \geq 0 \quad (3.13)$$

There exists a symmetric positive definite matrix  $\mathbf{P}$  satisfying:

$$\mathbf{A}_m^T \mathbf{P} + \mathbf{P} \mathbf{A}_m = -\mathbf{Q} \quad (3.14)$$

From Eq. (3.10) ~ Eq. (3.14), taking time derivative of  $V$  yields:

$$\dot{V} = -\mathbf{e}^T \mathbf{Q} \mathbf{e} + 2\Delta k_x \left( \mathbf{e}^T \mathbf{P} \mathbf{b} \mathbf{x} + \frac{\dot{\hat{\mathbf{k}}}_x^T}{\gamma_1} \right) + 2\Delta k_r \left( \mathbf{e}^T \mathbf{P} \mathbf{b} \theta_{ref} + \frac{\dot{\hat{\mathbf{k}}}_r}{\gamma_2} \right) \quad (3.15)$$

The proof of Eq. (3.15) is shown in Appendix A.

Substituting the adaption update law Eq. (3.12) into Eq. (3.15), the time derivative becomes:

$$\dot{V} = -\mathbf{e}^T \mathbf{Q} \mathbf{e} \leq 0 \quad (3.16)$$

This implies that  $e$ ,  $\Delta k_x$ ,  $\Delta k_r$  are bounded from Eq. (3.13) and Eq. (3.16) under the condition of Eq. (3.9) and Eq. (3.12). So the conditional stability of the closed-loop system is satisfied.

### 3.3 Reference model output signal

The control law of Eq. (3.9), consists of system state vector  $\mathbf{x}$  and the desired angular position as control voltage signal  $\theta_{ref}$ . One control input law such as the controller signal  $u$  is used for creating torque of Eq. (3.4) to track the reference model output. The most MRAC schemes uses the output of the reference model system  $y_m$  and the desired signal  $\theta_{ref}$  is preferred for such application. Based on this point of view, the reference motion and the corresponding voltage should be generated. A simple method is implemented by the transfer function of the reference model of Eq. (3.6), which is expressed by the transfer function [37] as follows:

$$G_m = C(SI - A_m)^{-1} b_m = \frac{\theta_m}{\theta_{ref}} = \frac{\omega_n^2}{s^2 + 2\zeta\omega_n s + \omega_n^2} \quad (3.17)$$

$$\theta_d = G_m \theta_{ref} \quad (3.18)$$

where  $\theta_{ref}(s)$  and  $\theta_d(s)$  are the Laplace from of  $\theta_{ref}$  and  $\theta_d$ , respectively.  $\theta_d$  is the reconstructed reference signal.  $\omega_n$  and  $\zeta$  are the undamped natural frequency and the damping ratio, which are used for determining  $A_m$  and  $b_m$  by setting the minimum parameters  $\omega_n$  and  $\zeta$ . The block diagram of the proposed MRAC scheme is shown in Fig. 3.10 [38].

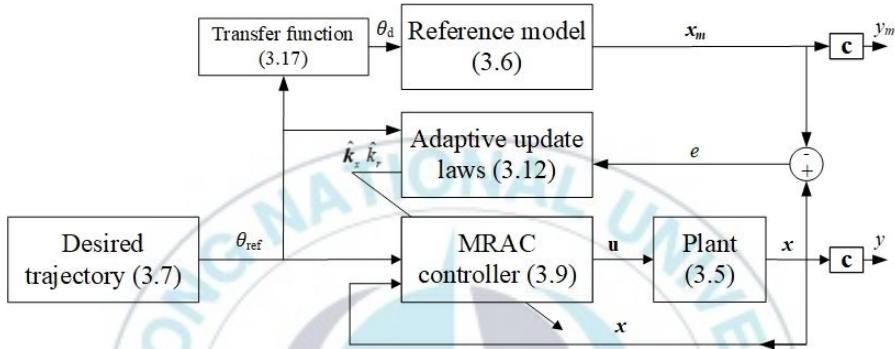


Fig. 3.3 Block diagram of the proposed MRAC scheme

### 3.4 Simulation results

The proposed controller design of the fish conveyor system belt based on the MRAC method is presented in section 3.2 and section 3.3. The simulation results using the proposed controller are shown in Fig. 3.4 ~ Fig. 3.8 under initial values of state variable and controller input as follows:

- The initial input voltage  $u(0)=0V$ ,  $a_0 = 0.333$ ,  $\theta_c = 0.333$  rad, the natural frequency  $\omega_n = 4.583$  rad/s and the damping ratio

$\zeta = 2.182$ , the initial update control law coefficient  $\hat{k}_{x1}(0) = -0.23$  V/rad,  $\hat{k}_{x2}(0) = -0.23$  Vs/rad and  $\hat{k}_r(0) = 0.62$  V/rad.

- The dynamic equation of the fish conveyor belt system is a second-order differential equation. The parameters of the dynamic equation, the adaption learning gain value and the transfer function are chosen  $a_{21m} = -21, a_{22m} = -20, b_{21m} = 21$ ,  $\gamma_1 = 0.035, \gamma_2 = 0.000001$  and  $G_m = \frac{21}{s^2 + 20s + 21}$ , respectively by the trial and error method.

Fig. 3.4 shows that the output of the reference model tracks the given reference step of 3.33 rad and the output of the fish conveyor belt system (MRAC) tracks the output of the reference model. The output of the fish conveyor belt system increases rapidly and follows the output reference and crosses over output reference at 8.5s. A changing point at 10 seconds is at the changing point from ramp signal to step signal. The output plant is not stable at the changing point. Maximum output reaches 3.51 rad at approximately 10.8 seconds and overshoot of 0.18 rad is shown. At 15 seconds, the plant output is stable and tracking desired position.

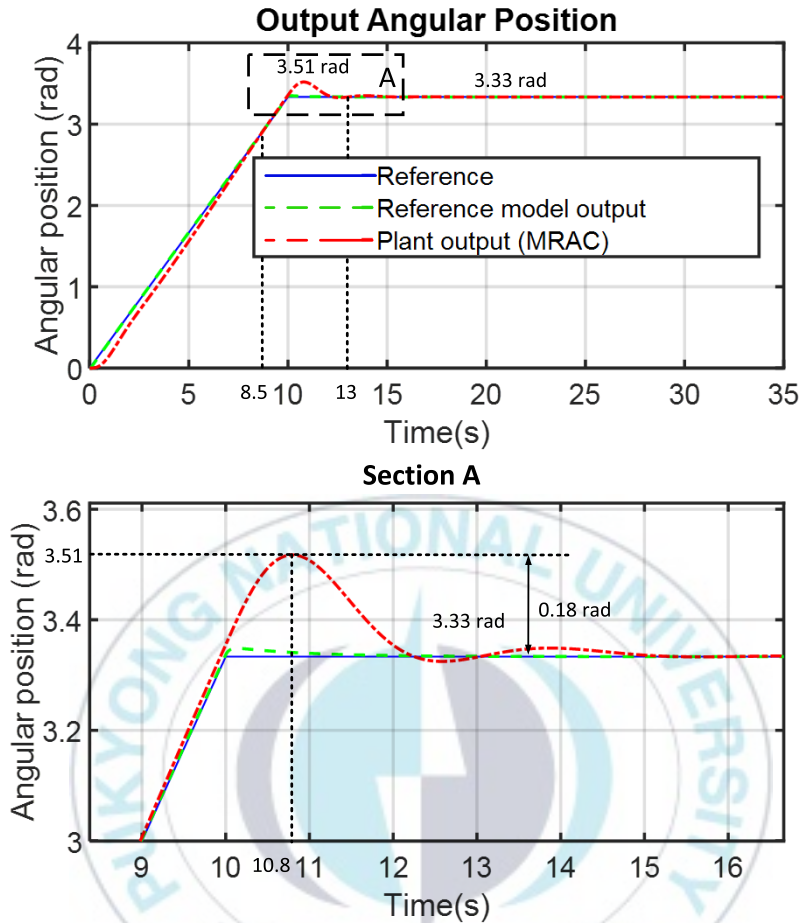


Fig. 3.4 Output angular position of MRAC control

The tracking error between angular position of reference model and desired angular position and the modeling error between angular position of reference model and plant output (MRAC) are shown on Fig. 3.5. It shows that the modeling error and the tracking error go to zero after 15 seconds clearly by the proposed controller. The plant output (MRAC) shows the modeling error of angular position  $-0.171$  rad at the beginning time of 1 second. At changing point, maximum value of the tracking error of reference model is  $0.015$  rad and maximum modeling error of output plant is about  $0.176$  rad at  $10.8$



seconds. The modeling error of angular position goes to 0 rad after 15 seconds. The modeling error of angular velocity is -0.32 rad/s at the beginning time and then goes to 0.05 rad/s. At changing point, maximum value of modeling error of angular velocity is 0.325/s rad at 10 seconds and then goes to 0 rad/s after 15 seconds.

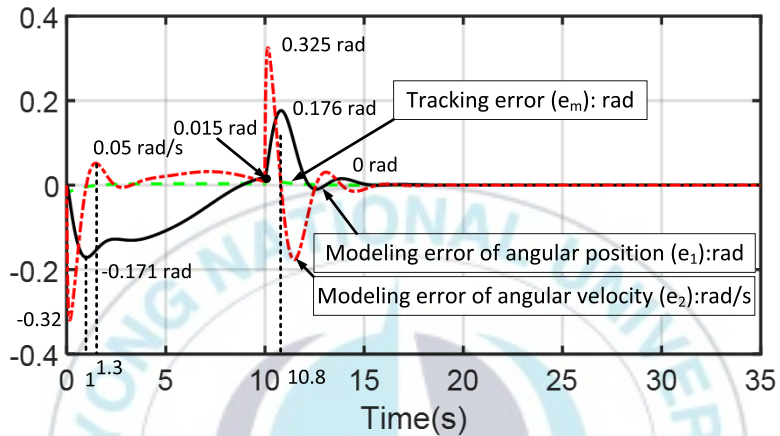


Fig. 3.5 Tracking error and modeling error

Fig. 3.6 ~ Fig. 3.8 illustrate the voltage control input, the update control law coefficient of system and the output angular velocity of MRAC control. The voltage control input peak at 1.4V at changing point and then converges to 1.3V often 11.17 seconds in Fig. 3.6.

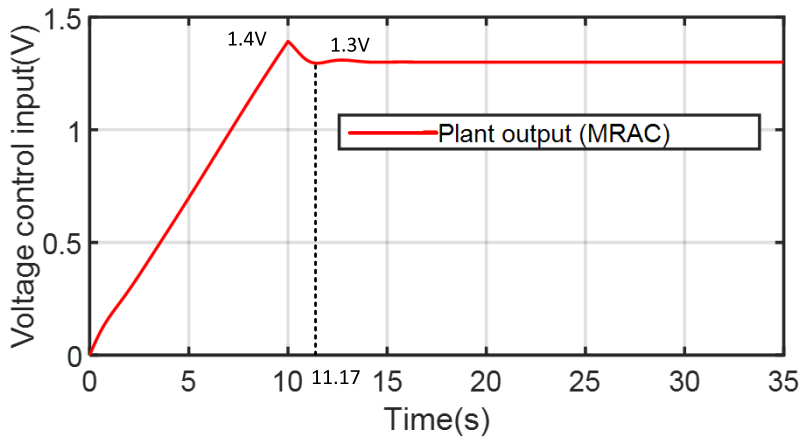


Fig. 3.6 Voltage control input signal

In Fig. 3.7,  $k_r$  is stable at 0.62 V/rad in during operating time. Likewise,  $k_{x1}$  peaks at -0.2V/rad at 10 seconds and then converges to -0.28 V/rad at 11.5 seconds.  $k_{x2}$  reaches at -0.135 Vs/rad at 6.8 seconds and then converge to -0.26 Vs/rad at 12 seconds.

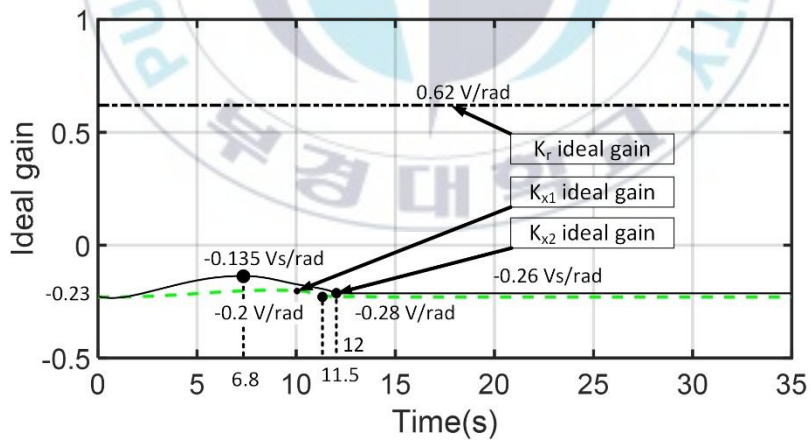


Fig. 3.7 Ideal gains for update control law

The angular velocity of MRAC control reaches maximum value approximately 0.4 rpm at 1.45 seconds and then goes to minimum value -0.18 rpm at 11.45 seconds. The output angular velocity of MRAC control converges to zero at 15 seconds in Fig. 3.8.

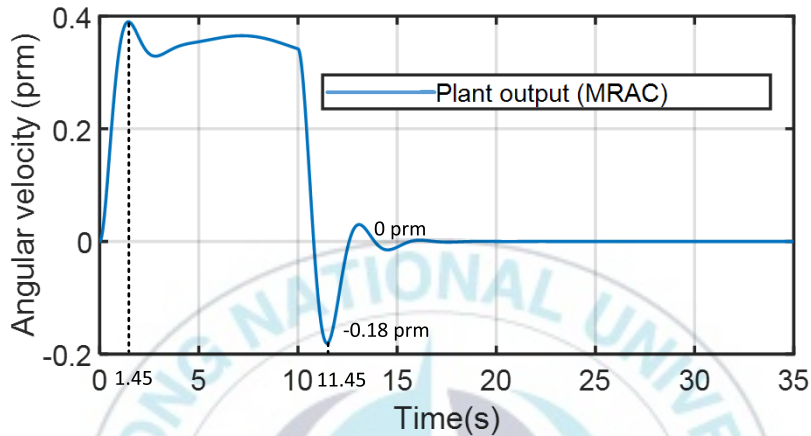


Fig. 3.8 Angular velocity

### 3.5 Summary

In this chapter, a model reference adaptive control (MRAC) method to control angular position of the fish conveyor belt system was proposed. The output of the reference model tracked the given desired step reference with the magnitude of 3.33 rad at 15 seconds and the output of the fish conveyor belt system (MRAC) tracked the output of the reference model. Maximum output angular position reached 3.51 rad at approximately 10.8 seconds. After 15 seconds output angular position converged to zero. Therefore, the system was stable and tracked a desired right position of camera center. Moreover, the angular velocity of MRAC converged to zero at 15 seconds.

## Chapter 4: MEASUREMENT OF INJURY RATE ON FISH SKIN BASED ON $L^*a^*b^*$ AND HSV COLOR SPACES

### 4.1 Image processing based on $L^*a^*b^*$ color space compared with HSV color space

$L^*a^*b^*$  color space is defined by CIE and specified by the International Commission on Illumination[39].

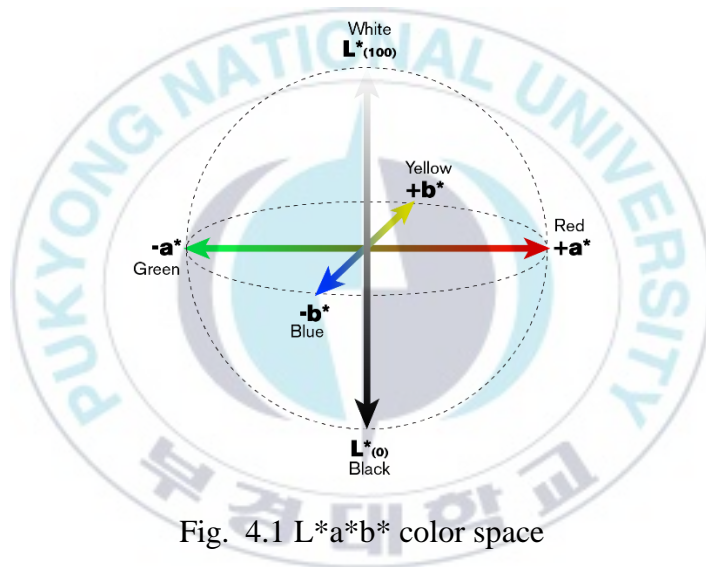


Fig. 4.1  $L^*a^*b^*$  color space

In Fig. 4.1, lightness ( $L^*$ ) is the central vertical axis which have range of value from 0 to 100 (black to white). The coordinate axes follows channel “ $a^*$ ”. If value of channel “ $a^*$ ” is a positive value, color of channel “ $a^*$ ” is red. If value is negative, color of channel “ $a^*$ ” is green. Channel “ $b^*$ ” is similar to channel “ $a^*$ ”. Positive value is yellow and negative value is blue.

In this case, the ZED stereo camera takes 8-bit RGB color images. RGB color space obtained by the ZED stereo camera is converted to L\*a\*b\* color space as follows:

The values of  $R$ ,  $G$ , and  $B$  are converted to the floating-point format and scaled to fit the 0 to 1 range as follows:

$$\begin{bmatrix} X \\ Y \\ Z \end{bmatrix} = \begin{bmatrix} 0.412453 & 0.357580 & 0.180423 \\ 0.212671 & 0.715160 & 0.072169 \\ 0.019334 & 0.119193 & 0.950227 \end{bmatrix} \begin{bmatrix} R \\ G \\ B \end{bmatrix} \quad (4.1)$$

$$X = \frac{X}{X_n}, \text{ where } X_n = 0.950456$$

$$Z = \frac{Z}{Z_n}, \text{ where } Z_n = 1.088754$$

$$L = \begin{cases} 116Y^{1/3} - 16 & \text{for } Y > 0.008856 \\ 903.3Y & \text{for } Y \leq 0.008856 \end{cases} \quad (4.2)$$

$$\begin{aligned} a &= 500(f(X) - f(Y)) + \text{delta} \\ b &= 200(f(Y) - f(Z)) + \text{delta} \end{aligned} \quad (4.3)$$

where

$$f(t) = \begin{cases} t^{1/3} & \text{for } t > 0.008856 \\ 7.787t + 16/116 & \text{for } t \leq 0.008856 \end{cases}$$

and

$$\text{delta} = \begin{cases} 128 & \text{for 8-bit image} \\ 0 & \text{for floatingpoint image} \end{cases}$$

$0 \leq L \leq 100$ ,  $-127 \leq a \leq 127$  and  $-127 \leq b \leq 127$  are the ranges of the values of outputs.  $t$  is the mediate variable of  $X$ ,  $Y$  and  $Z$ .

The value are then converted into data type of 8-bit image as follows:

$$L^* = L \frac{255}{100}; a = a + 128; b = b + 128 \quad (4.4)$$

In Fig. 4.2, there are three dimensions such as Hue (H), Saturation (S) and Value (V) in **HSV color space**. The Hue is an angle in the range  $[0,2\pi]$ . Saturation describes the purity of that Hue. The light illumination is a percentage goes from 0 to 100 presented by Value.

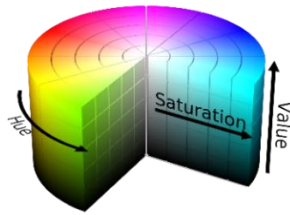


Fig. 4.2 HSV color space

In this section, an image processing algorithm based on  $L^*a^*b^*$  and HSV color spaces to determine the injury rate on fish surface is proposed as the flowchart in Fig. 4.3.

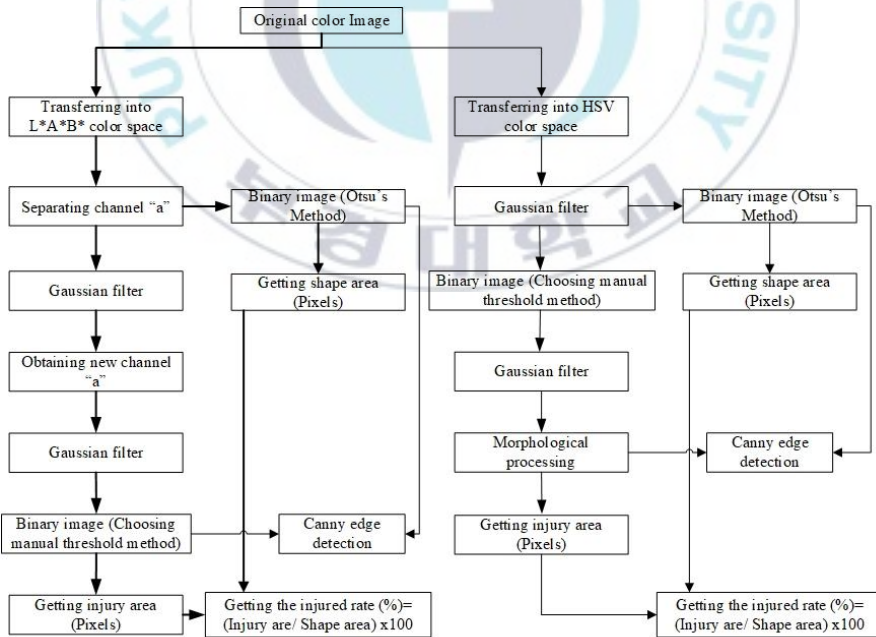


Fig. 4.3 Image processing algorithm for  $L^*a^*b^*$  color space and HSV color space

An original color image is captured by camera and transformed into L\*a\*b\* and HSV color spaces sequentially. After separating channel “a\*” from L\*a\*b\* color space, there are two tasks done in this image as follows:

Firstly, channel “a\*” is converted into binary image by Otsu's method. After that, area of the fish shape on the binary image is calculated by counting pixels.

Secondly, an adjusting method value of channel “a\*” is proposed to detect injury on fish clearly. The random noises of the original channel “a\*” image are reduced in this image by Gaussian filter. An image applying the adjusted value to the image filtered by Gaussian filter is called as a new channel “a\*” image.

The formula for adjusting value to the image filtered by Gaussian filter of channel “a\*” is as follows:

$$a_{new}(x, y) = h \frac{a(x, y)}{\max(a)} \quad (4.5)$$

where  $h$  is a coefficient which depends on conditional environment, and  $x$  and  $y$  is coordinate of pixels.

The new channel “a” image adjusted by Eq. (4.5) applies Gaussian filter to filter the rest of noises with Kernel coefficient chosen by manual. Next step, this image is converted into binary image by choosing a manual threshold method. The first Gaussian filter is applied to filter the random noises in this image converted into L\*a\*b\* color space and HSV color space. That is, the second Gaussian filter is applied to the images with Kernel coefficient chosen by manual.



**A binary image** is a digital image that has only two possible values for each pixel as shown in Eq. (4.6). Typically, the two colors used for a binary image are black and white. The color used for the objects in the image is the foreground color, while the rest of the image is the background color. This threshold operation can be expressed as [40]:

$$Binary\ value(x, y) = \begin{cases} 1 & \text{if } src(x, y) \geq thresh \\ 0 & \text{otherwise} \end{cases} \quad (4.6)$$

**Gaussian filter** is to blur an image by using Gaussian function for calculating the transformation to apply to each pixel in the image [41].

$$G_0(x, y) = Ae^{-\frac{(x-\mu_x)^2}{2\sigma_x^2} - \frac{(y-\mu_y)^2}{2\sigma_y^2}} \quad (4.7)$$

where  $\mu_x$  and  $\mu_y$  is the means, and  $\sigma_x$  and  $\sigma_y$  represent variances with respect to the variables  $x$  and  $y$ , respectively.

**Canny Edge detection algorithm** was developed by John F. Canny in 1986 [42]. Canny algorithm aims to follow the typical step: Gaussian filter, intensity gradient, double threshold and edge tracking by hysteresis [41].

**Morphology** is a broad set of image processing operations that process images based on shapes. Morphological operations apply a structuring element to an input image, creating an output image of the same size [41].

By counting the area pixels of injury and fish shape, an injury rate of fish surface is determined:

$$Injury\ rate = \frac{injury\ area\ (pixels)}{shape\ area\ (pixels)} \times 100\% \quad (4.8)$$

Finally, the Canny edge detection is used on injuries and fish shape on  $L^*a^*b^*$  and HSV color spaces to compare and to be sure show clearly the difference the results between  $L^*a^*b^*$  and HSV color spaces.

## 4.2 Experiment results

An original color image of fish in Fig. 4.4 is converted into  $L^*a^*b^*$  and HSV color spaces in Fig. 4.5 and Fig. 4.6, respectively. The original channel “a\*” image of fish is separated from  $L^*a^*b^*$  color space as shown in Fig. 4.7. Fig. 4.8 shows the new channel a\* image adjusting value of the original channel “a\*” of fish using the proposed Eq. (4.5). The original channel “a\*” images of the fish shape is converted into binary image from by using Otsu’s Method. Likewise, the new channel “a\*” images of injuries and the fish are converted into binary images by choosing a manual threshold method using Eq. (4.6). Channel “a\*” of  $L^*a^*b^*$  color space is sensitive to the red color, so adjusting value of channel “a\*” helps clear realization of injury area on fish. All of the results are presented in Fig. 4.9 and Fig. 4.10.



Fig. 4.4 Original color image

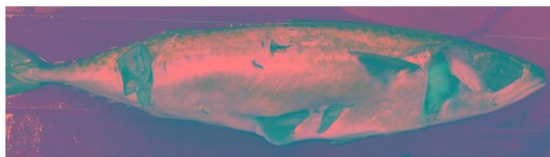


Fig. 4.5  $L^*a^*b^*$  color space image

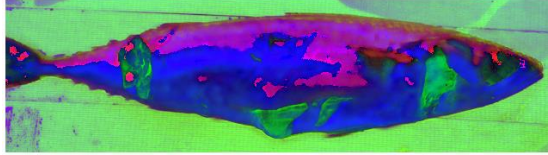


Fig. 4.6 HSV color space image

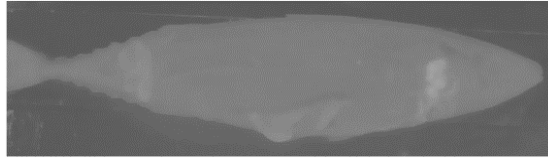


Fig. 4.7 Original channel "a\*" image on L\*a\*b\* color space



Fig. 4.8 New channel "a\*" image on L\*a\*b\* color space



Fig. 4.9 Binary image fish shape on L\*a\*b\* color space



Fig. 4.10 Binary injury image on L\*a\*b\* color space

The image processing of HSV color space is similar to that of L\*a\*b\* color space. The results are presented in Fig. 4.11 - Fig. 4.13. The results of counting pixels on areas of binary images of shape and injuries, and their injury rates based on L\*a\*b\* color space and HSV color space are shown in Table 4.1.



Fig. 4.11 Binary injury image on HSV color space before morphological processing



Fig. 4.12 Binary image fish shape on HSV color space



Fig. 4.13 Binary injury image on HSV color space after morphological processing



Fig. 4.14 Edge detection injuries and shape on fish image on HSV color space



Fig. 4.15 Edge detection injuries and shape on fish image on L\*a\*b\* color space

**Table 4.1:** Experiment results of the proposed algorithm (Pixels)

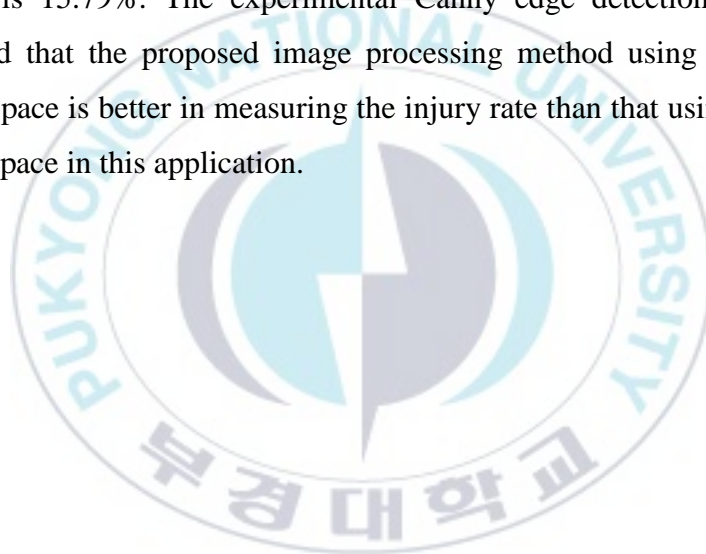
Object	L*a*b* color space	HSV color space	Real data
Shape	55492	55580	57323
Injury Object 1	2111	231	1947
Injury Object 2	1319	2264	1209
Injury Object 3	552	1974	573
Injury Object 4	2772	351	1742
Injury Object 5	-	23	-
Injury Object 6	-	3562	-
Total Injury Object	6754	8779	5471
Injury rate	12.17%	15.79%	9.54%

Finally, the injury rate based on areas of shape and total injuries of fish is calculated by Eq. (4.8). The proposed algorithms are tested by practical experiment on fish. There are four injury objects of the fish on L\*a\*b\* color space as shown in Fig. 4.10, while there are six injury objects on HSV color space as shown in Fig. 4.13. It means that process of image processing is effected by “noise” HSV color space. The injury rate of fish using L\*a\*b\* and HSV color spaces is 12.17% and 15.79% on Table 4.1, respectively. The injury rate using the proposed image processing algorithm based on L\*a\*b\* color space is 12.17% and is close to the real injury rate of 9.54% than that of based on HSV color space. Fig. 4.14 and Fig. 4.15 show that the edge of injuries and body for L\*a\*b\* color space is closer to the original image

than that for HSV color space after using Canny edge detection to compare.

### 4.3 Summary

In this chapter, comparison in performance using  $L^*a^*b^*$  and HSV color spaces and measurement of injury rate on fish surface were presented. By using the proposed image processing algorithm based on  $L^*a^*b^*$  color space, the injury rate is 12.17% and close to the real injury rate of 9.54%. Whereas, the injury rate based on HSV color space is 15.79%. The experimental Canny edge detection results showed that the proposed image processing method using  $L^*a^*b^*$  color space is better in measuring the injury rate than that using HSV color space in this application.



## Chapter 5: DETERMINATION OF INJURY RATE ON FISH SURFACE BASED ON FUZZY C-MEANS CLUSTERING ALGORITHM

### 5.1 Proposed injury rate measurement method on fish surface

In this section, an image processing algorithm based on  $L^*a^*b^*$  color space combined with the Fuzzy C-means clustering algorithm to obtain the injury rate of fish is presented. An original color full HD image is captured by ZED stereo camera, which is cropped to extract of an image of the fish body. Median and Bilateral filters are applied to filter white, salt-pepper and random noises due to environmental light on the cropped color image.

**Median filter** runs through each element of the image and replaces each pixel's value with the median of its neighboring pixels. This method is more powerful in dealing with "salt and pepper noise" [41]:

$$b[x, y] = \text{median}\{a[i, j], (i, j) \in w\} \quad (5.1)$$

where  $w$  represents a neighborhood defined by an user and  $a[i, j]$  is neighborhood of elements in the coordinate  $(i, j)$ .  $b[x, y]$  is the center location of the image.

**Bilateral filter** not only dissolves noise but also smooths edges, which makes edges less sharp and even disappear. Bilateral filter is more advanced and powerful than Gaussian filter as follows [41]:

$$g(i, j) = \sum_{k,l} f(i+m, j+l)h(m, l) \quad (5.2)$$



where  $g(i, j)$  is an output pixel's value,  $f(i+m, j+l)$  is an input pixel value and  $h(m, l)$  is a coefficient of filter at position  $(m, l)$  and called the kernel.

The cropped image is transformed into  $L*a*b*$  color space after it is filtered by median and bilateral filters. Fuzzy C-means clustering algorithm is applied directly on an  $L*a*b*$  image. The Fuzzy C-means clustering algorithm using on  $L*a*b*$  color space image is an iterative data-partitioning method. The Fuzzy C-means clustering algorithm uses the following [32]:

$$J_p = \sum_{i=1}^D \sum_{j=1}^N \mu_{ij}^p \|x_i - c_j\|^2 \quad (5.3)$$

where  $J_p$  is an objective function to be minimized.  $D$  is the number of data points.  $N$  is the number of clusters.  $p$  is the fuzzy partition matrix exponent for controlling the degree of fuzzy overlap, with  $p > 1$ .  $x_i$  is the  $i^{\text{th}}$  data point.  $c_j$  is the center of the  $j^{\text{th}}$  cluster.  $\mu_{ij}$  is the degree of membership of  $x_i$   $i^{\text{th}}$  cluster.

Fuzzy C-means clustering performs the following steps during clustering:

1. Randomly initialize the cluster membership values.
2. Calculate the cluster centers.

$$c_j = \frac{\sum_{i=1}^D \mu_{ij}^p x_i}{\sum_{i=1}^D \mu_{ij}^p} \quad (5.4)$$

3. Update  $\mu_{ij}$  according to the following:

$$\mu_{ij} = \frac{1}{\sum_{k=1}^N \left( \frac{\|x_i - c_j\|}{\|x_i - c_k\|} \right)^{\frac{2}{p-1}}} \quad (5.5)$$

4. Calculate the objective function.
5. Repeat steps 2-4 until  $J_p$  has converged to a local minimum.

On the line 1 of Fig. 5.1, original channel “a” is separated from  $L^*a^*b^*$  color space combined with the Fuzzy C-means clustering algorithm. For next step, a method to adjust value of channel “a” is used to detect injury on fish clearly. An image applying the adjusted value to the original channel “a” is called as a new channel “a” image. The formula for adjusting value of channel “a” is as follows [41]:

$$g(i, j) = \alpha \cdot f(i, j) + \beta \quad (5.6)$$

where  $g(i, j)$  is the output image pixels, and  $f(i, j)$  is the source image pixels. The parameters  $\alpha > 0$  and  $\beta$  are often called the gain and bias parameters chosen based on experiment of a user.

The new channel “a” is processed by the Fuzzy C-means clustering algorithm, and adjusting value of channel “a” improves accuracy of detecting injury on fish. Because the original channel “a” image is processed by the Fuzzy C-means clustering algorithm and its value is adjusted, this generates many random noises in the image. Before the new channel “a” image is transferred into binary image by Otsu’s method, it is filtered by Gaussian filter to reduce the random noises. This step is done from Eq. (5.1) to Eq. (5.6).

After that, the injury binary image is filtered by Median filter to filter salt-pepper noises which is generated in the previous step. This step follows Eq. (5.1). Counting pixels method is applied on injury binary image to count the sum of pixels of injury areas. The total pixels of injury areas are calculated as follows:

$$Injury \ area = \sum_{i=0}^{max \ i} \sum_{j=0}^{max \ j} x(i, j) \quad (pixels) \quad (5.7)$$

where  $max \ i$  is the height of image, and  $max \ j$  is the width of image.  $x(i, j)$  is pixel point in injury areas for the coordinate  $(i, j)$ .

On the line 2 of Fig. 5.1, original channel “b” is separated from  $L*a*b*$  color space combined with the Fuzzy C-means clustering algorithm. Before the channel “b” image is converted into binary image by Otsu’s method, the channel “b” image is filtered by Gaussian and Median filters, respectively. This steps follow Eq. (4.7), Eq. (5.1) and Eq. (5.2). Gaussian and Median filters filter the random noises which are generated in the previous step. An image is filtered by Median filter similarly to channel “a” in line 1. After that, area’s value of the body on the binary image is calculated by counting pixels. The total pixels of the fish body is calculated as follows:

$$Body \ area = \sum_{i=0}^{max \ i} \sum_{j=0}^{max \ j} x(i, j) \quad (pixels) \quad (5.8)$$

where  $max \ i$  is the height of image and  $max \ j$  is the width of image.  $x(i, j)$  is a pixel point of the body areas for the coordinate  $(i, j)$ .

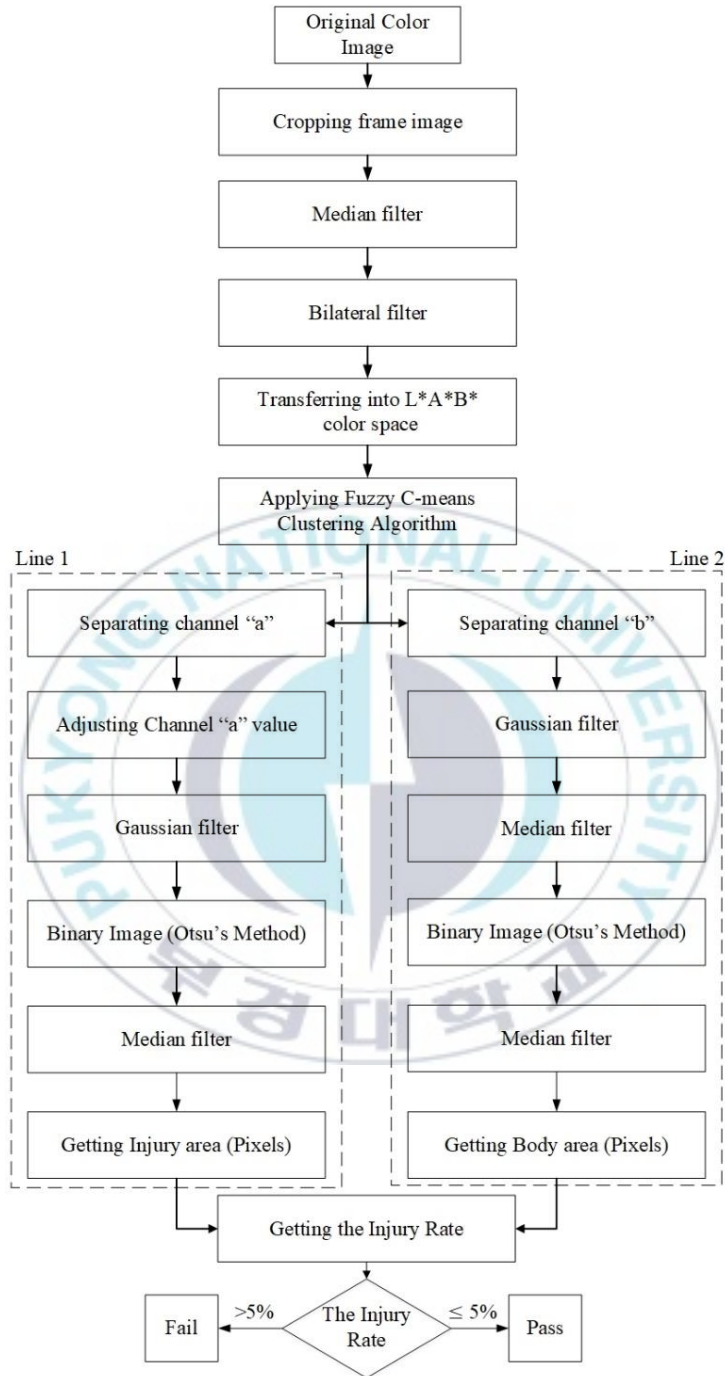


Fig. 5.1 Flowchart of the proposed image processing method

Finally, by counting the area pixels of injury and shape of fish, an injury rate of fish is calculated by Eq. (4.8) in chapter 4.

**Pass** is defined when the injury rate of fish is equal to and less than 5%, and **Fail** is defined in the opposite case.

To compare more clearly between the K-means clustering algorithm and the Fuzzy C-means clustering algorithm, the image processing flowchart is done with the same steps in Fig. 5.1.

**The K-means clustering algorithm** is the simplest algorithm that solve the well known clustering problem. This algorithm aims at minimizing an objective function as follows [32]:

$$J = \sum_{j=1}^z \sum_{i=1}^n \|x_i^{(j)} - c_j\|^2 \quad (5.9)$$

where  $\|x_i^{(j)} - c_j\|^2$  is distance measure between a data point  $x_i^{(j)}$  and the cluster center  $c_j$ ,  $n$  is data points.  $J$  is the minimizing objective function.

The K-means clustering performs the following steps:

1. Randomly initialize the cluster membership values  $z$ .
2. Assign each object to the group that has the closet centroid.
3. To recalculate the positions of the centroids.
4. To repeat step 2 and step 3 until the centroids no move.

## 5.2 Experiment results

An original full HD color image is captured by ZED camera, and then the image is processed by the flow chart in Fig. 5.1 and all steps are presented in the section 5.1. There are two samples which are tested by the proposed image processing method. The experimental results of sample 1 are shown in Fig. 5.2 ~ Fig. 5.9. The experimental results of sample 2 are shown in Fig. 5.10 ~ Fig. 5.18. Fish surface image processed data includes original fish tissue and injured data. In Fig. 5.2 and Fig. 5.10, injury parts have overlapped data with fish body image, only median and bilateral filters cannot determine whether the pixels of the overlapped data belong to fish body or injury areas. However, the overlapped data problem at injury parts is solved by applying Fuzzy C-means clustering algorithm shown as Fig. 5.3 and Fig. 5.11 with green color rectangle areas by minimizing the value of overlapped pixels.



Fig. 5.2 Cropped image from ZED stereo camera of sample 1 filtered by Median and Bilateral filter



Fig. 5.3 Fuzzy C-means clustering algorithm combined with  $L^*a^*b^*$  color space image of sample 1



Fig. 5.4 Original channel “a” image of sample 1

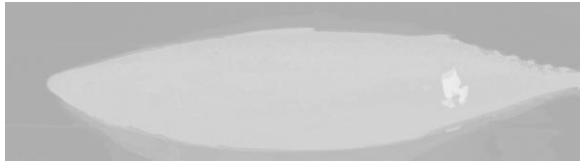


Fig. 5.5 New channel “a” image of sample 1

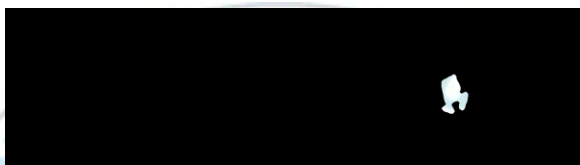


Fig. 5.6 Binary injury image of sample 1 filtered by Median filter



Fig. 5.7 Channel “b” image of sample 1 filtered by Gaussian filter



Fig. 5.8 Binary body image of sample 1



Fig. 5.9 Binary body image of sample 1 filtered by Median filter





Fig. 5.10 Cropped image from ZED stereo camera of sample 2 filtered by Median and Bilateral filter

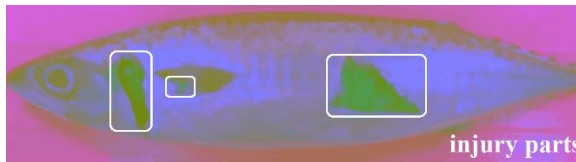


Fig. 5.11 Fuzzy C-means clustering algorithm combined with L\*a\*b\* color space image of sample 2



Fig. 5.12 Original channel "a" image of sample 2



Fig. 5.13 New channel "a" image of sample 2



Fig. 5.14 Binary injury image of sample 2 filtered by Median filter

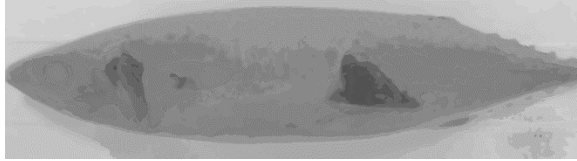


Fig. 5.15 Channel “b” image of sample 2

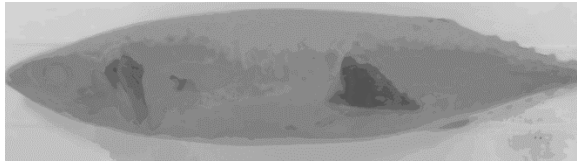


Fig. 5.16 Channel “b” image of sample 2 filtered



Fig. 5.17 Binary body image of sample 2



Fig. 5.18 Binary body image of sample 2 after filtered by Median filter

The results of the K-means clustering algorithm are shown in Fig. 5.19 ~ Fig. 5.21 for sample 1 and Fig. 5.22 ~ Fig. 5.24 for sample 2:



Fig. 5.19 K-means clustering algorithm combined with L\*a\*b\* color space image of sample 1

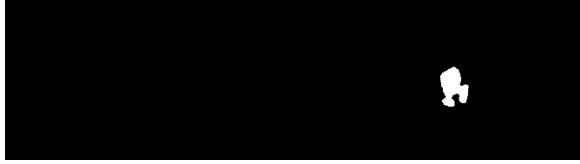


Fig. 5.20 Binary injury image of sample 1 filtered by Median filter (K-means)



Fig. 5.21 Binary body image of sample 1 filtered by Median filter (K-means)



Fig. 5.22 K-means clustering algorithm combined with L\*a\*b\* color space image of sample 2



Fig. 5.23 Binary injury image of sample 2 filtered by Median filter (K-means)



Fig. 5.24 Binary body image of sample 2 filtered by Median filter (K-means)

**Table 5.1:** Experimental results of the injury rate (Pixels).

Object		Body	Total injury area	Injury rate	Testing
Proposed process	Sample 1	279239	4076	1.46%	Pass
	Sample 2	355422	26866	7.56%	Fail
K-means process	Sample 1	278483	4428	1.59%	Pass
	Sample 2	352245	26313	7.47%	Fail
Real data	Sample 1	287344	4256	1.48%	Pass
	Sample 2	369759	28756	7.78%	Fail

Finally, the injury rate of fish is calculated by body and total injury areas on fish based on Eq. (4.8) and is shown in Table 5.1. The proposed image processing method is tested by practical experiment on fishes that the injury rate of fishes is 1.46% in sample 1 and 7.56% in sample 2, respectively. The K-means clustering algorithm is tested on fishes that the injury rate of fishes is 1.59% in sample 1 and 7.47% in sample 2, respectively. The injury rate of the proposed image processing method is really close to real injury rate, which small gap is 0.02% in sample 1 and 0.22% in sample 2. Whereas, the gap between the real injury rate and the injury rate measured by the K-means clustering algorithm is 0.11% in sample 1 and 0.31% in sample 2.

### 5.3 Summary

This chapter proposed the an image processing system designed and an image processing method based on L\*a\*b\* color space combined with the Fuzzy C-means clustering algorithm using ZED stereo camera

to measure injury rate on fish surface. By calculating the pixels of areas of body and total injury, the injury rate were calculated. The proposed image processing method solved the overlapped problem that could not determine whether the overlapped data belong to fish body or injury parts. Moreover, several kind of filters such as Median, Bilateral and Gaussian filters were used in the proposed image processing method to filter several different type of noises to improve accuracy of the injury rate. The injury rate using the Fuzzy C-means clustering algorithm was 1.46% in sample 1 and 7.56% in sample 2 close to the real injury rate of 1.48% and 7.78%, respectively. Whereas, the injury rate using the K-means clustering algorithm was 1.59% in sample 1 and 7.47% in sample 2. The experimental results verified that the injury rate measured by the proposed image processing method was closer to the real injury rate than that of the K-means clustering algorithm. The injury rate of fish in sample 1 was less than 5% as “Pass” and sample 2 was large than 5% as “Fail”.

## Chapter 6: CONCLUSIONS AND FUTURE WORKS

### 6.1 Conclusions

This thesis proposed an angular position controller based on MRAC for a fish conveyor belt system to determine of injury rate on fish surface using an image processing. The image processing method was applied to select or remove the injured fishes based on the permissive injury rate using ZED stereo camera. The conclusions of this thesis were summarized as follows:

- **In chapter 2:** The mechanical and electronic structure of a fish conveyor belt system was designed and explained in detail. The proposed image processing system included camera, lamps, computer, the image processing box and cover, which were also described and manufactured.

- **In chapter 3:** System modeling was described to design an angular position controller for a fish conveyor belt system under several unmeasurable parameters. A model reference adaptive controller (MRAC) was presented for a SISO system. All parameters in the fish conveyor belt system were an estimated by the MRAC. The stability of the proposed controller is analyzed by Lyapunov stability theory and Barbalat's lemma. The output of the reference model tracked the given desired step reference with the magnitude of 3.33 rad at 15 seconds and the output of the fish conveyor belt system (MRAC) tracked the output of the reference model. After 15 seconds output angular position converged to zero. Maximum value of the tracking error of reference model is 0.015 rad and maximum modeling error of

output plant is about 0.176 rad at 10.8 seconds. The modeling error of angular position goes to 0 rad after 15 seconds. Maximum value of modeling error of angular velocity is 0.325/s rad at 10 seconds and then goes to 0 rad/s after 15 seconds. Therefore, the system was stable and tracked a desired right position of camera center.

- **In chapter 4:** A performance using  $L^*a^*b^*$  and HSV color spaces and measurement of injury rate on fish surface were proposed. For the experimental results using the proposed image processing algorithm based on HSV color space, the injury rate was 15.79% and, the injury rate based on  $L^*a^*b^*$  color space was 12.17%. The result of  $L^*a^*b^*$  color space was closer to the real injury rate of 9.54% than that of HSV color space. So the experimental results showed that the proposed image processing algorithm using  $L^*a^*b^*$  color space was better in measuring the injury rate than that using HSV color space. The edge of injuries and body for  $L^*a^*b^*$  color space is closer to the original image than that for HSV color space after using Canny edge detection to compare.

- **In chapter 5:** An image processing algorithm using  $L^*a^*b^*$  color space and the Fuzzy C-means clustering algorithm using a ZED stereo camera to measure injury rate on fish surface was proposed. The proposed image processing method solved the overlapped problem that could not determine whether the overlapped data belonged to fish body or injury parts. The injury rate using the Fuzzy C-means clustering algorithm was 1.46% in sample 1 and 7.56% in sample 2 close to the real injury rate of 1.48% and 7.78%, respectively. Whereas, the injury rate using the K-means clustering algorithm was 1.59% in sample 1 and 7.47% in sample 2. So the experimental results verified that the

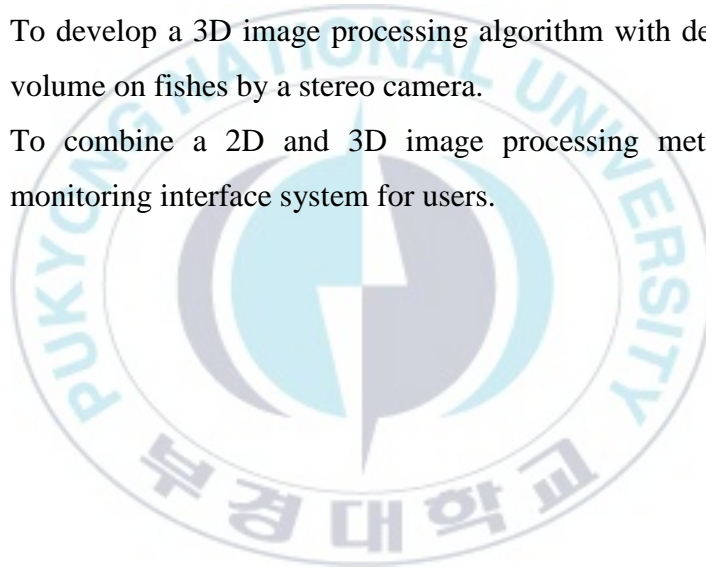


injury rate measured by the proposed image processing algorithm was closer to the real injury rate than that by the K-means clustering algorithm. The permissive injury rate is 5%. The injury rate of fish in sample 1 was less than permissive injury rate as “Pass” and that in sample 2 was large than permissive injury rate as “Fail”.

## 6.2 Future works

As for this thesis, the future works will be made as follows:

- To apply a robust controller.
- To develop a 3D image processing algorithm with depth and volume on fishes by a stereo camera.
- To combine a 2D and 3D image processing method for monitoring interface system for users.



## REFERENCES

- [1] M. C. Tsai and C. H. Lee, "Tracking Control of a Conveyor Belt: Design and Experiments", *IEEE Transactions on Robotics and Automation*, vol. 12, no. 1, pp. 126-131, 1996.
- [2] T. H. Nguyen, D. B. Sheng, T. S. Gao, H. K. Kim and S. B. Kim, "Application of Servo Controller Design Method for Speed Control of a Belt Driven Transmission Section in a Fish Sorting Conveyor System", Korean Society for Precision Engineering (KSPE), Korea, 2016.
- [3] H. H. Nguyen, "Development of Velocity Controllers for Induction Conveyor Line in a Cross-Belt Sorter System", *Ph.D. Thesis*, Mechanical Design Engineering, Pukyong National University, Pukyong National University, 2017.
- [4] A. A. A. El-Gammal and A. A. El-Samahy, "A Modified Design of PID Controller For DC Motor Drives Using Particle Swarm Optimization PSO", International Conference on Power Engineering, Energy and Electrical Drives 2009, Lisbon, Portugal, 2009.
- [5] E. Lavretsky and K. A. Wise, *Robust and Adaptive Control*. Springer, 2013.
- [6] K. J. Astrom and B. Wittenmark, *Adaptive Control*. Addison Wesley Publishing Company, 1995.
- [7] K. K. Ahn, D. N. C. Nam and M. Jin, "Adaptive Backstepping Control of an Electrohydraulic Actuator", *IEEE/ASME Transaction on Mechatronics*, vol. 19, no. 3, pp. 987-995, 2014.
- [8] M. Sunwoo, K. C. Cheok and N. J. Huang, "Model Reference Adaptive Control for Vehicle Active Suspension Systems",

- IEEE Transactions On Industrial Electronics*, vol. 38, no. 3, pp. 217-222, 1991.
- [9] S. M. Joshi, G. Tao and P. Patre, "Direct Adaptive Control Using An Adaptive Reference Model", *International Journal of Control*, vol. 84, no. 1, pp. 180-196, 2011.
- [10] V. Stepanyan and K. Kalmanje, "Input and Output Performance of M-MRAC in the Presence of Bounded Disturbances", AIAA Guidance, Navigation, and Control Conference, Guidance, Navigation, and Control and Co-located Conferences, Toronto, Canada, August 2010.
- [11] M. Kanamori and M. Tomizuka, "Model Reference Adaptive Systems with Input Control of Linear Saturation", International Conference on Control Applications, Taipei, Taiwan, September, 2004.
- [12] A. Das and F. L. Lewis, "Cooperative adaptive control for synchronization of second-order systems with unknown nonlinearities", *International Journal of Robust and Nonlinear Control*, vol. 21, pp. 1509–1524, 2010.
- [13] N. A. Valous and D. W. Sun, *Computer Vision Technology in the Food and Beverage Industries*. Woodhead Publishing, 2012.
- [14] D. J. Bora and A. K. Gupta, "A Novel Approach Towards Clustering Based Image Segmentation", *International Journal of Emerging Science and Engineering (IJESE)*, vol. 2, no. 11, pp. 6-10, 2014.
- [15] D. J. Bora and A. K. Gupta, "A New Approach towards Clustering based Color Image Segmentation", *International*

- Journal of Computer Applications*, vol. 107, no. 12, pp. 23-30, 2014.
- [16] S. Dhameliya, J. Kakadiya and R. Savant, "Volume Estimation of Mango", *International Journal of Computer Applications*, vol. 143, no. 12, pp. 11-16, 2016.
- [17] D. J. White, C. Svellingen and N. J. C. Strachan, "Automated measurement of species and length of fish by computer vision", *Fisheries Research*, vol. 80, no. 2006, pp. 203-210, 2006.
- [18] D. J. Bora, A. K. Gupta and F. A. Khan, "Comparing the Performance of L\*A\*B\* and HSV Color Spaces with Respect to Color Image Segmentation", *International Journal of Emerging Technology and Advanced Engineering*, vol. 5, no. 2, pp. 192-203, 2015.
- [19] S. Sural, G. Qian and S. Pramanik, "Segmentation And Histogram Generation Using The Hsv Color Space For Image Retrieval", IEEE International Conference on Image Processing, New York, USA, 2002.
- [20] I. L. Weatherall and B. D. Coombs, "Skin Color Measurements in Terms of CIELAB Color Space Value", *The Society for Investigative Dermatology*, vol. 99, no. 4, pp. 468-473, 1991.
- [21] K. Leon, D. Mery, F. Pedreschi and J. Leo, "Color Measurement in L\*a\*b\* Units from RGB Digital Images", *Food Research International*, vol. 39, no. 2006, pp. 1084-1091, 2006.
- [22] I. Markovic, J. Ilic, D. Markovic, V. Simonovic and N. Kosanic, "Color Measurement Of Food Products Using CIE L\*a\*b\*

- And RGB Color Space", *Journal of Hygienec Engineering and Design*, vol. 4, no. 4, pp. 50-53, 2013.
- [23] V. S. Rathore, M. S. Kumar and A. Verma, "Colour Based Image Segmentation Using L\*A\*B\* Colour Space Based On Genetic Algorithm", *International Journal of Emerging Technology and Advanced Engineering*, vol. 2, no. 6, pp. 156-162, 2012.
- [24] R. A. Itle and E. A. Kabelka, "Correlation Between L\*a\*b\* Color Space Values and Carotenoid Content in Pumpkins and Squash", *HortScience*, vol. 44, no. 3, pp. 633–637, 2009.
- [25] V. E. Nambi, K. Thangavel, S. Shahir and V. Geetha, "Evaluation of Colour Behavior During Ripening of Banganapalli Mango Using CIE-Lab and RGB Colour Coordinates", *Journal of Applied Horticulture*, vol. 17, no. 3, pp. 205-209, 2015.
- [26] P. Crnosija, Z. Ban and R. Krishnan, "Overshoot Controlled Servo System Synthesis Using Bode Plot and Its Application to PM Brushless DC Motor Drive", 7th International Workshop on Advanced Motion Control, Maribor, Slovenia, July 2002.
- [27] P. Crnosija, R. Krishnan and T.Bjazic, "Transient Performance Based Design Optimization of PM Brushless DC Motor Drive Speed Controller", The IEEE International Symposium on Industrial Electronics, Dubrovnik, Croatia, 2005.
- [28] P. Panwar, G. Gopal and R. Kumar, "Image Segmentation Using K-means Clustering and Thresholding", *International*

- Research Journal of Engineering and Technology (IRJET)*, vol. 3, no. 5, pp. 1787-1793, 2016.
- [29] H. Chakravorty, R. Paul and P. Das, "Image Processing Technique To Detect Fish Disease", *International Journal of Computer Science & Security*, vol. 9, no. 2, pp. 121-131, 2015.
- [30] D. B. Sheng, S. B. Kim, T. H. Nguyen, T. S. Gao and H. K. Kim, "Fish Injured Rate Measurement Using Color Image Segmentation Method Based on K-Means Clustering Algorithm and Otsu's Threshold Algorithm", *Journal of the Korean Society for Power System Engineering*, vol. 19, no. 2, pp. 64-68, 2015.
- [31] Z. Cebeci and F. Yildiz, "Comparison of K-means and Fuzzy C-means Algorithms on Different Cluster Structures", *Journal of Agricultural Informatics*, vol. 6, no. 3, pp. 13-23, 2015.
- [32] A. Sheshasayee and P. Sharmila, "Comparative Study of Fuzzy C-means and K-means Algorithm for Requirements Clustering", *Indian Journal of Science and Technology*, vol. 7, no. 6, pp. 853-857, 2014.
- [33] D. B. Sheng, S. B. Kim, D. Dhayfole, T. S. Gao and H. K. Kim, "Analysis of Injured Rate Using Color Image Segmentation Based on K-means Clustering Algorithm", Korean Society for Precision Engineering (KSPE), Korea, 2016
- [34] Mitsubishi Electric, "Inverter Instruction Manual (Basic)", M. E. Corporation, Ed., 2002.
- [35] ZED SDK, "ZED SDK User Guide v2.0.1", StereoLABS, Ed., 2017.

- [36] R.S. Khurmi and J. K. Gupta, *A Textbook of Mechine Design*. S Chand & Co Ltd, 2005.
- [37] D. Graham and R. C. Lathrop, "The Synthesis of "Optimum" Transient Response: Criteria and Standard Forms", *Trans AIEE*, vol. 1953, no. 72, pp. 273-288, November 1953.
- [38] M. S. Tran *et al.*, "Model Reference Adaptive Control Strategy for Application to Robot Manipulators", The 5th International Conference on Advanced Engineering - Theory and Applications 2018, Ostrava, Czech, 2018.
- [39] R. S. Hunter, "Photoelectric Color Difference Meter", *Journal of The Optical Society of America*, vol. 48, no. 12, pp. 985-995, 1958.
- [40] N. Otsu, "A Threshold Selection Method from Gray-Level Histograms", *IEEE Transactions On Systems*, vol. 9, no. 1, pp. 62-66, 1979.
- [41] OpenCV Community, "The OpenCV Tutorials Release 2.4.13.2," OpenCV, Ed., 2017.
- [42] J. Canny, "A Computational Approach to Edge Detection", *IEEE Transactions on Pattern Analysis and Machine Intelligence*, vol. Pami-8, no. 6, pp. 679-698, 1986.



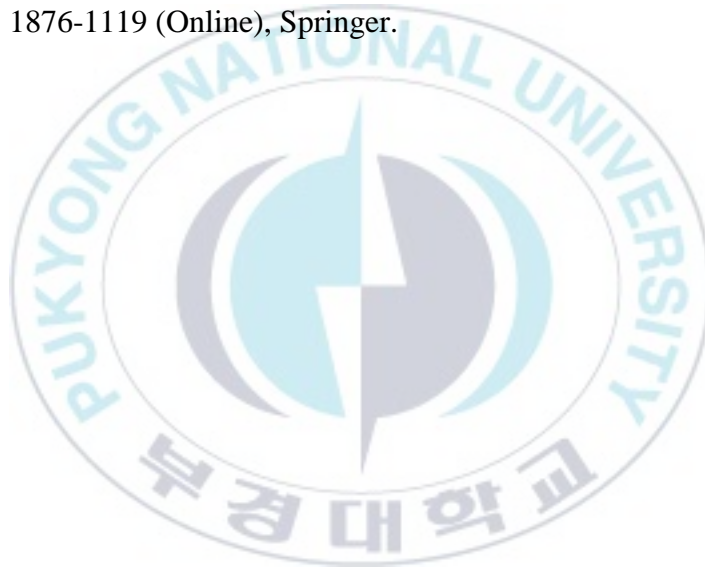
## PUBLICATIONS AND CONFERENCE

### Published Journal

1. **Minh Thien Tran**, Huy Hung Nguyen, Jotje Rantung, Hak Kyeong Kim, Sea June Oh and Sang Bong Kim, "A New Approach of 2D Measurement of Injury Rate on Fish by a Modified K-means Clustering Algorithm Based on L\*A\*B\* Color Space", *Recent Advances in Electrical Engineering and Related Sciences, Lecture Notes in Electrical Engineering*, vol. 465, pp. 324-333, 2017. **SCOPUS**, ISSN 1876-1110 (Print), / ISSN 1876-1119 (Online), Springer.
2. **Minh Thien Tran**, Jotje Rantung, Trong Hai Nguyen, Hak Kyeong Kim and Sang Bong Kim, "Measurement of Injury Rate on Fish Skin and Performance Comparison Based on L\*A\*B\* and HSV Color Space", *MATEC Web of Conferences*, vol. 159, pp. 1-6, 2018. **SCOPUS**, / ISSN 2261-236X (Online).
3. Huy Hung Nguyen, **Minh Thien Tran**, Dae Hwan Kim, Hak Kyeong Kim and Sang Bong Kim, "Velocity Controller Design for Fish Sorting Belt Conveyor System Using M-MRAC and Projection Operator", *Journal of the Korean Society for Power System Engineering*, vol. 21, no. 4, pp. 42-50, 2017. **KOREA**, ISSN 1226-7813 (Print), / ISSN 2367-1354 (Online).
4. Huy Hung Nguyen, **Minh Thien Tran**, Dae Hwan Kim, Hak Kyeong Kim and Sang Bong Kim, "Fault Detection Algorithm for a Velocity Controller Using MRAC in the Belt Conveyor System of a Fish Processing Line", *Journal of Institute of Control, Robotics and System*, vol. 24, no. 2, pp. 149-154, 2018.

**SCOPUS**, ISSN 1976-5622 (Print), / ISSN 2233-4335 (Online).

5. Jotje Rantung, **Minh Thien Tran**, Hwan Yeol Jang, Jin Woo Lee, Hak Kyeong Kim and Sang Bong Kim, "Determination of the Fish Surface Area and Volume Using Ellipsoid Approximation Method Applied for Image Processing", *Recent Advances in Electrical Engineering and Related Sciences, Lecture Notes in Electrical Engineering*, vol. 465, pp. 334-347, 2017. **SCOPUS**, ISSN 1876-1110 (Print), / ISSN 1876-1119 (Online), Springer.



## Conference Paper

1. **Minh Thien Tran**, Dae Hwan Kim, Chang Kyu Kim, Hak Kyeong Kim and Sang Bong Kim, "Determination of Injury Rate on Fish Surface Based on Fuzzy C-means Clustering Algorithm and L\*a\*b\* Color Space Using ZED Stereo Camera", *15<sup>th</sup> International Conference on Ubiquitous Robot 2018 (URAI) proceeding*, Hawaii, USA, pp.472-477, 2018, **IEEE (Online)**.
2. **Minh Thien Tran**, Jotje Rantung, Trong Hai Nguyen, Hak Kyeong Kim and Sang Bong Kim, "Measurement of Injury Rate on Fish Skin and Performance Comparison Based on L\*A\*B\* and HSV Color Space", *The 2nd International Joint Conference on Advanced Engineering and Technology (IJCAET 2017) and International Symposium on Advanced Mechanical and Power Engineering (ISAMPE 2017) proceeding*, Bali, Indonesia, pp. 72, 2017.

## Appendix A: Proof of Eq. (3.15)

$$V = \mathbf{e}^T \mathbf{P} \mathbf{e}$$

$$\dot{V} = \dot{\mathbf{e}}^T \mathbf{P} \mathbf{e} + \mathbf{e}^T \mathbf{P} \dot{\mathbf{e}}$$

$$\begin{aligned} &= \left[ \mathbf{A}_m \mathbf{e} + \mathbf{b} (\Delta \mathbf{k}_x^T \mathbf{x} + \Delta k_r \theta_{ref}) \right]^T \mathbf{P} \mathbf{e} + \mathbf{e}^T \mathbf{P} \left[ \mathbf{A}_m \mathbf{e} + \mathbf{b} (\Delta \mathbf{k}_x^T \mathbf{x} + \Delta k_r \theta_{ref}) \right] \\ &= (\mathbf{A}_m \mathbf{e})^T \mathbf{P} \mathbf{e} + \left[ \mathbf{b} (\Delta \mathbf{k}_x^T \mathbf{x} + \Delta k_r \theta_{ref}) \right]^T \mathbf{P} \mathbf{e} + \mathbf{e}^T \mathbf{P} \mathbf{A}_m \mathbf{e} + \mathbf{e}^T \mathbf{P} \mathbf{b} (\Delta \mathbf{k}_x^T \mathbf{x} + \Delta k_r \theta_{ref}) \\ &= \mathbf{A}_m^T \mathbf{e}^T \mathbf{P} \mathbf{e} + (\mathbf{P} \mathbf{e})^T \mathbf{b} (\Delta \mathbf{k}_x^T \mathbf{x} + \Delta k_r \theta_{ref}) + \mathbf{e}^T \mathbf{P} \mathbf{A}_m \mathbf{e} + \mathbf{e}^T \mathbf{P} \mathbf{b} (\Delta \mathbf{k}_x^T \mathbf{x} + \Delta k_r \theta_{ref}) \\ &= \mathbf{e}^T (\mathbf{A}_m^T \mathbf{P} + \mathbf{P} \mathbf{A}_m) \mathbf{e} + \mathbf{e}^T \mathbf{P}^T \mathbf{b} (\Delta \mathbf{k}_x^T \mathbf{x} + \Delta k_r \theta_{ref}) + \mathbf{e}^T \mathbf{P} \mathbf{b} (\Delta \mathbf{k}_x^T \mathbf{x} + \Delta k_r \theta_{ref}) \\ &= \mathbf{e}^T (\mathbf{A}_m^T \mathbf{P} + \mathbf{P} \mathbf{A}_m) \mathbf{e} + 2 \mathbf{e}^T \mathbf{P} \mathbf{b} (\Delta \mathbf{k}_x^T \mathbf{x} + \Delta k_r \theta_{ref}) \end{aligned}$$

$$\mathbf{A}_m^T \mathbf{P} + \mathbf{P} \mathbf{A}_m = -\mathbf{Q}$$

$$V = \mathbf{e}^T \mathbf{P} \mathbf{e} + \frac{\Delta \mathbf{k}_x^T \Delta \mathbf{k}_x}{\gamma_1} + \frac{\Delta k_r^2}{\gamma_2} \geq 0 \quad (\gamma_1, \gamma_2 > 0)$$

$$\begin{aligned} \dot{V} &= -\mathbf{e}^T \mathbf{Q} \mathbf{e} + 2(\mathbf{e}^T \mathbf{P} \mathbf{b}) (\Delta \mathbf{k}_x^T \mathbf{x} + \Delta k_r \theta_{ref}) + \frac{2 \Delta \mathbf{k}_x^T}{\gamma_1} \dot{\Delta \mathbf{k}_x} + \frac{2 \Delta k_r}{\gamma_2} \dot{\Delta k_r} \\ &= -\mathbf{e}^T \mathbf{Q} \mathbf{e} + 2(\mathbf{e}^T \mathbf{P} \mathbf{b}) (\Delta \mathbf{k}_x^T \mathbf{x} + \Delta k_r \theta_{ref}) + \frac{2 \Delta \mathbf{k}_x^T}{\gamma_1} \dot{\mathbf{k}}_x + \frac{2 \Delta k_r}{\gamma_2} \dot{k}_r \\ &= -\mathbf{e}^T \mathbf{Q} \mathbf{e} + 2(\mathbf{e}^T \mathbf{P} \mathbf{b}) (\Delta \mathbf{k}_x^T \mathbf{x}) + 2(\mathbf{e}^T \mathbf{P} \mathbf{b}) (\Delta k_r \theta_{ref}) + \frac{2 \Delta \mathbf{k}_x^T}{\gamma_1} \dot{\mathbf{k}}_x + \frac{2 \Delta k_r}{\gamma_2} \dot{k}_r \\ &\quad (\because \mathbf{e}^T \mathbf{P} \mathbf{b} \text{ and } \Delta \mathbf{k}_x^T \mathbf{x} \text{ are scalar}) \\ &= -\mathbf{e}^T \mathbf{Q} \mathbf{e} + 2(\Delta \mathbf{k}_x^T \mathbf{x})(\mathbf{e}^T \mathbf{P} \mathbf{b}) + 2(\Delta k_r \theta_{ref})(\mathbf{e}^T \mathbf{P} \mathbf{b}) + \frac{2 \Delta \mathbf{k}_x^T}{\gamma_1} \dot{\mathbf{k}}_x + \frac{2 \Delta k_r}{\gamma_2} \dot{k}_r \\ &= -\mathbf{e}^T \mathbf{Q} \mathbf{e} + 2 \Delta \mathbf{k}_x^T \left( \mathbf{x} (\mathbf{e}^T \mathbf{P} \mathbf{b}) + \frac{\dot{\mathbf{k}}_x}{\gamma_1} \right) + 2 \Delta k_r \left( \theta_{ref} (\mathbf{e}^T \mathbf{P} \mathbf{b}) + \frac{\dot{k}_r}{\gamma_2} \right) \leq 0 \\ &\Rightarrow \begin{cases} \dot{\mathbf{k}}_x = -\gamma_1 (\mathbf{e}^T \mathbf{P} \mathbf{b}) \mathbf{x} \\ \dot{k}_r = -\gamma_2 (\mathbf{e}^T \mathbf{P} \mathbf{b}) \theta_{ref} \end{cases} \\ \dot{V} &= -\mathbf{e}^T \mathbf{Q} \mathbf{e} \leq 0 \end{aligned}$$